Journal of Medicinal Chemistry

pubs.acs.org/jmc

Article

# Phorbol Diesters and 12-Deoxy-16-hydroxyphorbol 13,16-Diesters Induce TGFα Release and Adult Mouse Neurogenesis

Abdellah Ezzanad, Ricardo Gómez-Oliva, Felipe Escobar-Montaño, Mónica Díez-Salguero, Noelia Geribaldi-Doldan, Samuel Dominguez-Garcia, José Manuel Botubol-Ares, Carolina de los Reyes, Rosa Durán-Patrón, Pedro Nunez-Abades, Antonio J. Macías-Sánchez, Carmen Castro, and Rosario Hernández-Galán*

Cite This: *J. Med. Chem.* 2021, 64, 6070−6084

Read Online

ACCESS | Metrics & More | Article Recommendations | Supporting Information

**ABSTRACT:** A small library of phorbol 12,13-diesters bearing low lipophilicity ester chains was prepared as potential neurogenic agents in the adult brain. They were also used in a targeted UHPLC−HRMS screening of the latex of *Euphorbia resinifera*. Two new 12-deoxy-16-hydroxyphorbol 13,16-diesters were isolated, and their structures were deduced using two-dimensional NMR spectroscopy and NOE experiments. The ability of natural and synthetic compounds to stimulate transforming growth factor alpha (TFGα) release, to increase neural progenitor cell proliferation, and to stimulate neurogenesis was evaluated. All compounds that facilitated TGFα release promoted neural progenitor cell proliferation. The presence of two acyloxy moieties on the tigliane skeleton led to higher levels of activity, which decreased when a free hydroxyl group was at C-12. Remarkably, the compound bearing isobutyryloxy groups was the most potent on the TGFα assay and at inducing neural progenitor cell proliferation *in vitro*, also leading to enhanced neurogenesis *in vivo* when administered intranasally to mice.

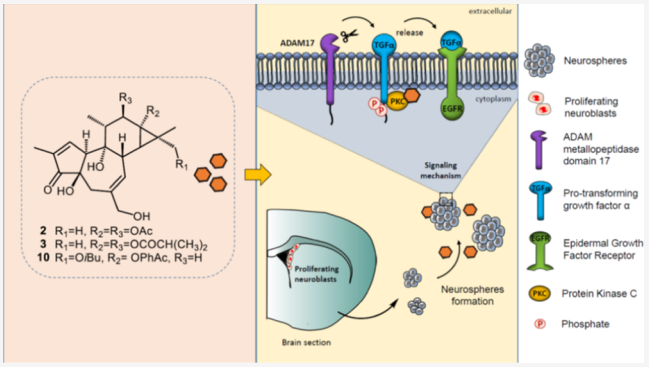


## INTRODUCTION

Brain damage caused by neurological and vascular disorders or by traumatic injuries is tightly associated with an irreversible neuronal loss, which may lead to cognitive impairment, motor dysfunction, and even alterations of the personality.[1−3] Despite the physiological capacity of the adult brain to generate new neurons from neural stem cells (NSC) in the subventricular zone (SVZ)[4] and the dentate gyrus (DG) of the hippocampus,[5] neuronal replacement in damaged brain regions rarely occurs, complicating functional recovery. An association of alterations in neurogenesis with cognitive impairment has been described in mouse models of different metabolic and neurological disorders,[6,7] and it is generally accepted that increased neurogenesis leads to improve cognitive performance.[8] Thus, this field demands the discovery of new drugs that regenerate damaged brain regions, facilitating functional recovery. Searching for molecules that potentiate the capacity of NSC to generate new neurons in the adult brain is a crucial step in this pathway.

Our group has previously shown that several phorbol derivatives such as 12-deoxyphorbol 13-acetate (Prostratin), phorbol 12-myristate-13-acetate (PMA), 12-deoxyphorbol 13-phenylacetate (DPP), 12-deoxyphorbol 13-isobutyrate (DPB), and 12-deoxyphorbol 13-angelate (DPA) (Supporting Information, Figure S1) are capable of inducing adult neural progenitor cell (NPC) proliferation *via* PKC activation and of stimulating neurogenesis in the adult brain neurogenic niche of the SVZ and DG. Particularly, it was found that the 12-deoxyphorbol isolated from *Euphorbia resinifera*, DPB, showed the highest capacity to stimulate neurogenesis *in vivo*.[9] Furthermore, the long-term intranasal administration of DPB exerted not only a potent effect in stimulating neurogenesis in both the SVZ and DG, but the treatment of mice with this compound also improved their capacity to perform memory and learning tasks.[10] The comparison of the activity of all 12-deoxyphorbols tested with DPB[9] pointed at the role of the C-13 acyl chains as a key element in defining the potency of these compounds at activating PKC and promoting neurogenesis *in vivo*. Additionally, unlike PMA, other 12-deoxyphorbols 13-acyl esters previously described[9] did not show tumorigenic

**Received:** January 27, 2021
**Published:** May 4, 2021

**Scheme 1. Synthesis of Monoacyl and Diacylphorbols**[a]

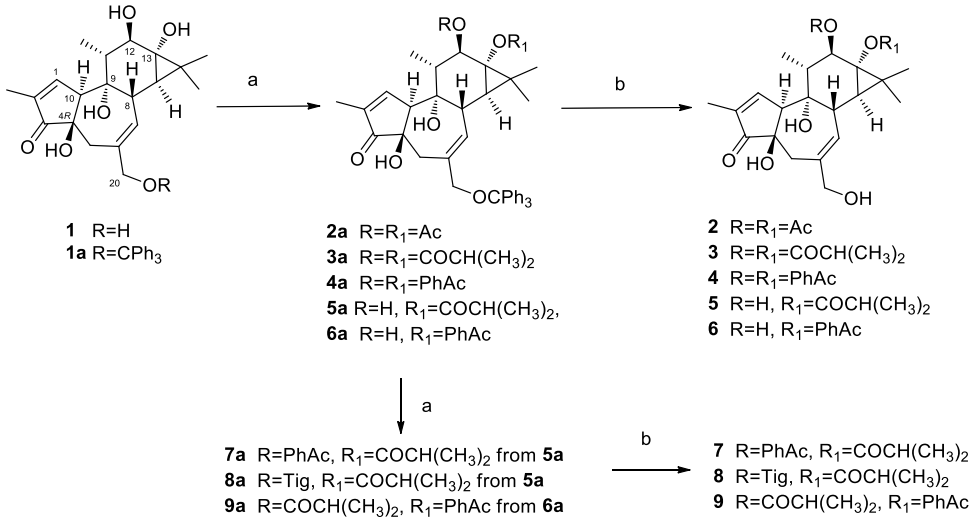


[a]Reagents and conditions: (a) $Ac_2O/C_5H_5N$, rt, 7 h for **2a** (99% yield); isobutyric acid, DMAP, EDCI, dichloromethane for **3a**, **5a**, and **9a** (99, 99, and 82%, respectively); phenylacetic acid, DMPA, EDCI, dichloromethane for **4a**, **6a**, and **7a** (82, 67, and 73% yield, respectively); tiglic acid, DMAP, EDCI, dichloromethane for **8a** (47% yield). (b) $HClO_4$, rt 30 min for **2**, **3**, **4**, **5**, and **6** (99, 87, 90, 84, and 86%, respectively); $HClO_4$, rt 15 min for **7**, **8**, and **9** (75, 79, and 52% yield, respectively).

activity, suggesting 12-deoxyphorbols 13-acyl esters as good candidates to produce potent pharmacological drugs that promote neurogenesis and facilitate functional repair of damaged brain tissue.

Regarding the mechanism of action of these phorbol derivatives, it has been reported that conventional PKC activation facilitates the secretion of neurotrophic factors that induce NPC proliferation such as the transforming growth factor alpha (TGF$\alpha$). This neurotrophic factor stimulates the proliferation of undifferentiated NPC by binding and activating the epidermal growth factor receptor (EGFR). PKC-mediated phosphorylation of membrane-bound pro-TGF$\alpha$ facilitates the ADAM17-mediated shedding of the soluble TGF$\alpha$ ligand.[11−13] Furthermore, it has been recently described that DPB elicits TGF$\alpha$ release mimicking the effect of TGF$\alpha$ in cultures of NPC.[10]

In this paper, we describe the preparation of selected phorbol 12,13-diesters (**2**−**9**) from commercial Croton oil, their use for identification of 12-deoxy-16-hydroxyphorbol 13,16-diesters through a screening-assisted ultrahigh performance liquid chromatography (UHPLC)−high-resolution mass spectroscopy (HRMS) from the latex of *E. resinifera* and also the isolation and characterization of two new 12-deoxy-16-hydroxyphorbol 13,16-diesters (**10**−**11**). Furthermore, we report the evaluation of these compounds as inducers of TGF$\alpha$ release, promoters of NPC expansion in the absence of epidermal growth factor, and as neurogenesis-stimulating small molecules. We also show structure−activity studies that can help the development of this class of compounds as effective neurogenic agents.

## RESULTS AND DISCUSSION

Among the 12-deoxyphorbol esters tested previously,[9,10] those with a phenylacetate or isobutyrate chain on C-13 (DPP and DPB, respectively) presented good activity at the lower range of tested concentrations. Therefore, it is reasonable to conceive that the nature of the biological activity of this class of compounds depends on the number and type of ester chains on the phorbol skeleton. Consequently, it is logical to consider that compounds with two ester functional groups, like PMA, but bearing less lipophilic chains, like those found in 12-deoxyphorbol esters such as the ones mentioned above, would present a better activity profile.

A review of the literature shows that not only phorbol esters at C-12 and C-13 have been described but also derivatives with no substituents at C-12, but with ester groups at C-13 and C-16 (12-deoxy-16-hydroxyphorbol 13,16-diesters).[14,15] Both groups of compounds would be related to 12-deoxyphorbols like those described above (Figure S1) but with an extra acyloxy chain either at C-12 or C-16.

Phorbol diesters bearing different chains at C-12 and C-13 could conceivably be prepared starting from a commercially available mixture of phorbols coming from Croton oil, an oil obtained from the seeds of *Croton tiglium*.[16] On the other hand, as no synthetic procedures have been described for the preparation of 12-deoxy-16-hydroxyphorbol 13,16-diesters, they would have to be obtained from natural sources. For instance, the presence of 12-deoxy-16-hydroxyphorbol derivatives in the latex of *E. resinifera*[17−19] is known.

With this in mind, we have prepared a small library of phorbols bearing low-lipophilicity ester chains through chemical transformations on C-20-protected phorbol obtained from Croton oil. Based on our previous results[9] and with the aim to evaluate the effect of the presence of an extra acyloxy moiety on the tigliane skeleton, we decided to prepare 12,13-diester-bearing acetate, phenylacetate, isobutyrate, and methylbutenoate chains (like prostratin, DPP, DPB, and DPA, respectively). To analyze the effect of an extra free hydroxyl group, and as DPB has resulted to be the most potent compound when tested as a neural precursor promoter,[9] phorbol 13-isobutyrate was also prepared. On the other hand, to study the impact of the location of the chain on the tigliane skeleton on the capability of induction of the NPC proliferation, mixed 12,13-diesters carrying a combination of these chains were prepared, and both groups of compounds were used to identify possible 12-deoxy-16-hydroxyphorbol


https://doi.org/10.1021/acs.jmedchem.1c00156
J. Med. Chem. 2021, 64, 6070−6084

13,16-diesters in the latex of *E. resinifera* through a targeted UHPLC−HRMS method. The exchange of chains between C-12 and C-13 could tell us if the activity was associated with the location of each chain in a specific position or simply with their presence in that area of the molecule. Finally, a comparison of the effect of diesters in 12,13 with those of 13,16-diesters would inform us about the influence of the relative position of the ester group on the tigliane skeleton.

**Synthesis of Phorbol Diesters.** A set of phorbol esters was prepared by selective transformations at C-12, C-13, and C-20 positions on the tigliane skeleton.

Reactivity of hydroxyl groups in phorbol (**1**) toward esterification proceeds in the order C-20 > C-13 > C-12 due to steric effects.[20] Therefore, to selectively acylate the hydroxyl groups on C12 and/or C13 of phorbol, the primary allylic alcohol at C20 must be first protected.

Croton oil was used as a source of phorbol (**1**), and a modified protocol reported by Bertolini et al.[20] was used to isolate phorbol 20-trityl ether (**1a**) (Supporting Information, Scheme S1). Once the hydroxyl group at C-20 was protected, we proceeded to functionalize C-12 and C-13 following a modification of the previously reported strategy.[20]

A hydrolysis reaction of the trityl ether allows the recovery of the hydroxyl group at C-20.

A careful chromatographic purification of precursor **1a** must be carried out in order to avoid the co-occurrence of the epimer at C-4 ((4*S*)-phorbol derivatives). Epimerization at C-4 can take place through a retro-aldol-mediated rearrangement in a basic medium.[21,22] Due to the conformational change associated with the epimerization at C-4, (4*S*)-phorbol derivatives are not PKC activators.[20]

20-Trityl phorbol esters containing identical chains at C-12 and C-13 (**2a**−**4a**) were obtained following the procedure shown in Scheme 1. While ester **2a** was obtained by treatment of **1a** with acetic anhydride in pyridine, esters **3a** and **4a** were prepared by treatment with either isobutyric or phenyl acetic acid, *N*-ethyl-*N*′-(3-dimethylaminopropyl) carbodiimide (EDCI) hydrochloride, and *N*,*N*-dimethylamino pyridine (DMAP) (Scheme 1). All attempts to obtain phorbol 12,13-diangelate were unsuccessful.

As mentioned above, the C-13 hydroxyl group in phorbol derivatives is more reactive toward esterification than the one at C-12.[20] Therefore, C-13 monoacyl esters **5a** and **6a** could be prepared in a similar fashion to **3a** and **4a**, modifying slightly the reaction conditions (Scheme 1). In order to achieve selective acylation on C-13, temperature control and close monitoring of the reaction using thin layer chromatography (TLC) are required.

Once selective conditions for the preparation of 13-acylphorbols were found, it was possible to prepare 12,13-diacylphorbols with different chains at C-12 and C-13. Consequently, 20-tritylphorbol 12-phenylacetate-13-isobutyrate (**7a**), 20-tritylphorbol 12-tigliate-13-isobutyrate (**8a**), and 20-tritylphorbol 12-isobutyrate-13-phenylacetate (**9a**) (Scheme 1) were prepared as they would incorporate at C-12 ester groups already present in bioactive 12-deoxyphorbols.[9] Treatment of **5a** with phenylacetic acid or tiglic acid yielded **7a** and **8a**. Diester **9a** was prepared, starting from **6a** by treatment with isobutyric acid (Scheme 1). Finally, hydrolysis of trityl group at C-20 was achieved by treatment of corresponding diacylphorbol derivatives (**2a**−**9a**) with $HClO_4$ (0.01 M) at room temperature for 30 min to produce compounds **2**−**9**.

**UHPLC−HRMS-Assisted Identification, Isolation, and Structural Elucidation of 12-Deoxyphorbol13,16-diesters from *E. resinifera*.** 12-Deoxy-16-hydroxyphorbol 13,16-diesters and phorbol 12,13-diesters with the same ester moieties are isomeric and, therefore, are expected to show equivalent molecular ions in mass spectrometry.

Consequently, using the chemical formula of compounds **2**−**9** as leads, extracted ion chromatograms (XIC) for pseudomolecular ions $[M + Na]^+$, in electrospray ionization (ESI) positive mode and $[M + HCOOH-H]^-$ in ESI negative mode, were obtained by the UHPLC−HRMS analysis of the fractions obtained from the column chromatography of the latex of *E. resinifera*, as described in the Experimental Section. XIC for *m*/*z* 575.2621 (calculated mass for $C_{32}H_{40}O_8Na$, corresponding to $[M + Na]^+$ for both compounds **7** and **9**) in ESI positive mode and *m*/*z* 597.2700 (calculated mass for $C_{33}H_{41}O_{10}$, corresponding to $[M + HCOOH-H]^-$ for both compounds **7** and **9**) in ESI negative mode provided chromatographic peaks with different retention times to those of compound **9**, under equivalent elution conditions (Supporting Information, Figures S36 and S37). Therefore, the *E. resinifera* fraction where the above mentioned compounds were detected, isomeric to **7** and **9**, was subject to a careful isolation procedure, as detailed in the Experimental Section, yielding compounds **10** and **11** (Figure 1). A comparison of

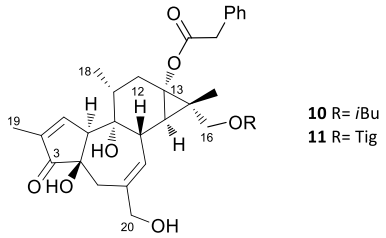


**Figure 1.** Structures of **10**−**11**.

the HRMS of the isomeric compounds **9**, **10**, and **11**, in ESI positive mode, and with a data-independent acquisition ($MS^E$), allowing the fragmentation of all ions within full *m*/*z* range,[23] shows similarities and some differences on both sets of spectra. $MS^E$ of these compounds shows a relatively abundant fragmentation corresponding to $[M\text{-PhAcOH-}(CH_3)_2CCO_2H + Na]^+$ (calculated *m*/*z* 351.1572).

Further fragmentations derived from this ion showed differences in compound **9**, on the one hand, and both compounds **10** and **11**, on the other, under equivalent $MS^E$ conditions (Figure 2 and Supporting Information, Schemes S2, S3, and S4). On the one hand, for compound **9**, a further loss of water (one and two molecules) and CO leads to ions *m*/*z* 311.1647, *m*/*z* 293.1541, and *m*/*z* 265.1592 (calculated). These are considered diagnostic fragments, associated with different mass spectrometry strategies to identify phorbol esters in complex mixtures.[24,25] On the other, for compound **10**, additional ions at *m*/*z* 323.1623, *m*/*z* 275.1436, and *m*/*z* 247.1487 (calculated) were observed, which were not apparent in the $MS^E$ of compound **9**. As detailed in the proposed fragmentation map for compound **10** (Figure 2 and Supporting Information, Scheme S3), while the ion at *m*/*z* 323.1623 could be explained by further loss of CO from the ion at *m*/*z* 351.1572, ions at *m*/*z* 275.1436 and *m*/*z* 247.1487 could be explained by further loss of water and CO, respectively, from *m*/*z* 293.1541 ($[M + H\text{-}2H_2O\text{-PhAcOH-}(CH_3)_2CCO_2H]^+$).


https://doi.org/10.1021/acs.jmedchem.1c00156
J. Med. Chem. 2021, 64, 6070−6084

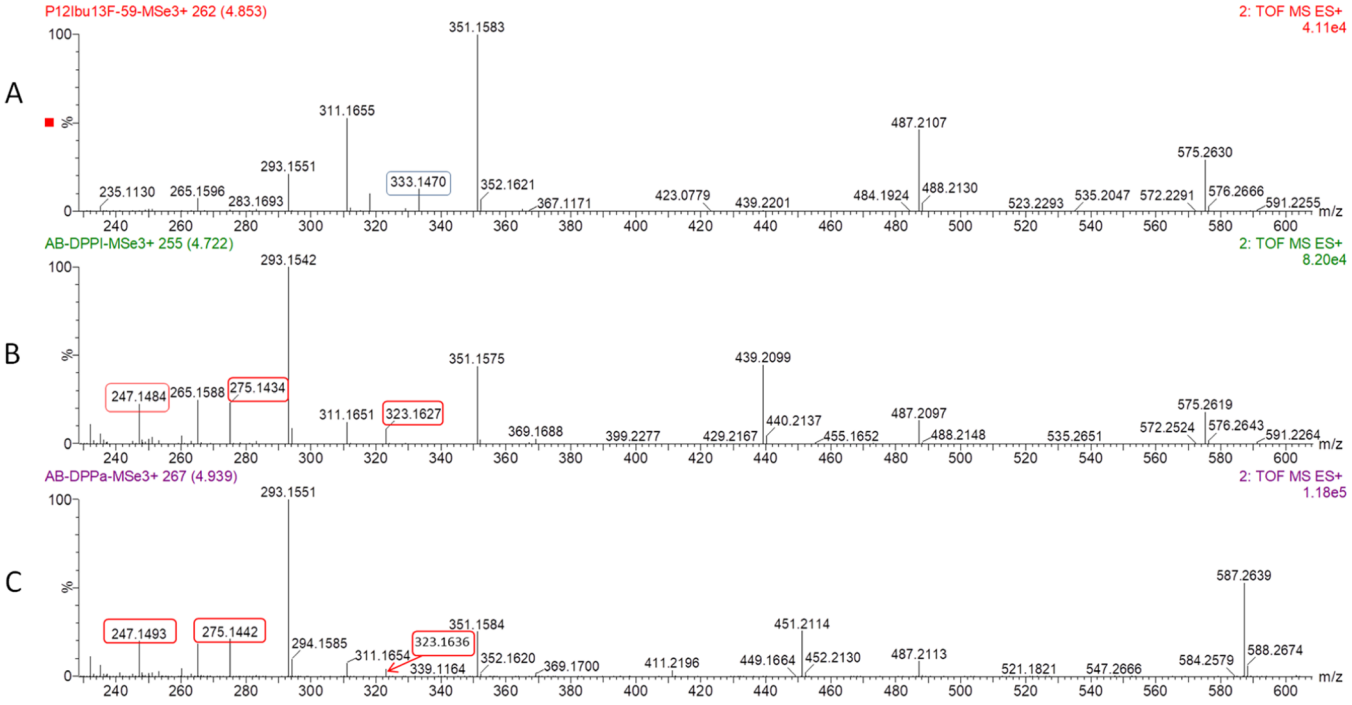


**Figure 2.** Comparison of $MS^E$ spectra (Data-Independent Acquisition)[20] for (A) compound **9**, (B) compound **10**, and (C) compound **11** (data acquired in positive ionization with a ramp tramp collision energy of the high-energy function set at 60−120 eV).

Interestingly, the latter fragmentation was the most abundant one observed in the ESI positive-ion mass spectra of compound **10** due to in-source fragmentations. Similar fragmentation patterns were observed for compound **11** (Figure 2 and Supporting Information, Scheme S4).

Comparison of the $^1$H and $^{13}$C NMR spectra, as well as heteronuclear multiple−bond correlation (HMBC) coupling patterns of **10**−**11** with those of **7**−**9**, indicates that the substituents were now located on C-13 and C-16 (Table 1).

The $^{13}$C NMR spectra of compounds **10** and **11** showed the presence of only three methyl groups and three methylenes, indicating that the substituent on C-12 on phorbol 12,13-diesters must be now located on one of the methyls of the *gem*-dimethyl group on C-15.$^1$H NMR data for **10**, and **11** showed the presence of phenylacetate (3.63, s, 7.31−7.23, m for **10** and 3.62, s, 7.32−7.19, m for **11**) and either an isobutyrate (2.53, sp; 1.15, d; 1.14, d for **10**) or a tigliate ester (6.84, q; 1.82, s; 1.81 d for **11**), respectively. The main difference between the $^1$H NMR spectra of the natural compounds **10** and **11** and those of the synthetic compounds was the presence of two doublets ($\delta_H$ 4.05 and 3.85 ppm in **10** and 4.14 and 3.84 ppm in **11**), which correlated to a methylene group ($\delta_C$ 70.2 and 70.5 ppm, respectively) in the gHSQC experiments. These methylene groups were assigned to C-16 because of their correlation with the carbon signals assigned to C-17 ($\delta_C$ 11.7 ppm in **10** and 11.8 ppm in **11**) in the gHMBC. The long-range couplings of the protons $H_2$-16 with the carbonyl carbons at $\delta_C$ 178.6 ppm in **10** and 169.5 ppm in **11** in the gHMBC spectra demonstrated that isobutyril and tiglyl groups are located at C-16. Consequently, phenylacetyl groups could only be located on the C-13 quaternary carbon. Furthermore, the presence of a methylene group at C-12 was confirmed by the correlations observed in the gHMBC experiments between the methyl groups at C-11 ($\delta_H$ 0.84 and 0.89 ppm, respectively) and the C-12 carbons in each compound. Nuclear Overhauser effect spectroscopy (NOESY) correlations observed for H-16$\alpha$, H-16$\beta$/H-14, and $H_3$-17/H-8, $H_3$-17/H-11 in all compounds (Supporting Information) confirmed that $H_2$-16 is $\alpha$-oriented, as H-14, and $H_3$-17 is $\beta$-oriented, as H-8 and H-11. Accordingly, compounds **10** and **11** were assigned as 12-deoxy-16-hydroxyphorbol 16-isobutyrate-13-phenyl acetate (DPPI) and 12-deoxy-16-hydroxyphorbol 13-phenylacetate-16-tigliate (DPPT), respectively. Both are new compounds and are described here for the first time.

**Effect of Phorbol Diesters and 12-Deoxy-16-hydroxyphorbol 13,16-Diesters on TGF$\alpha$ Release.** A previous report shows that 12-deoxyphorbol DPB stimulated neurogenesis and improved memory in mice by facilitating TGF$\alpha$ release and promoting the proliferation of NSC.[10] In order to analyze whether the compounds isolated and synthesized had the ability to facilitate the release of TGF$\alpha$, we built a fusion protein in which TGF$\alpha$ was expressed flanked by green fluorescent protein (GFP) and mCherry in the C-terminal and N-terminal domains, respectively (Figure 3B). This construct was transfected into HEK293T cells and the ratio mCherry/GFP in the cell membrane was quantified by using life imaging upon addition of the different compounds. By using this TGF$\alpha$ probe, cells expressing TGF$\alpha$ will show a 1:1 ratio of mCherry to GFP. However, if the shedding of TGF$\alpha$ occurs, cells will lose a percentage of mCherry fluorescence proportional to the amount of TGF$\alpha$ being released to the extracellular medium, whereas the GFP fluorescence will remain attached to the membrane. Thus, in the absence of shedding, the m-Cherry/GFP ratio remains unaltered, whereas the shedding and release of soluble TGF$\alpha$ should lower this ratio. As shown in Figure 3B,C, in the absence of compound (Ø; see Supporting Information, Movie 1) or in the presence of 0.5 $\mu$M phorbol (**1**; see Supporting Information, Movie 2), the mCherry/GFP ratio remains unaltered; however, the addition of compound **3** (see Supporting Information, Movie 3) and an identical


https://doi.org/10.1021/acs.jmedchem.1c00156
J. Med. Chem. 2021, 64, 6070−6084

**Table 1. Summary of NMR Data for DPPI (10) and DPPT (11)**

| | DPPI (**10**) | | DPPT (**11**) | |
|---|---|---|---|---|
| pos | $\delta_H$ (J in Hz)[a] | $\delta_C$[b] | $\delta_H$ (J in Hz)[c] | $\delta_C$[d] |
| 1 | 7.53, m | 160.8 | 7.53, m | 160.8 |
| 2 | | 135.0 | | 134.6 |
| 3 | | 210.5 | | 210.5 |
| 4 | | 74.7 | | 74.7 |
| 5 | 2.50, d (19.0) | 38.6 | 2.51, d (19.0) | 38.6 |
| | 2.42, d (19.0) | | 2.42, d (19.0) | |
| 6 | | 142.4 | | 142.4 |
| 7 | 5.56, bd (5.8) | 129.7 | 5.58, bd (5.7) | 129.6 |
| 8 | 3.08, t (5.8) | 39.3 | 3.10, t (5.7) | 39.3 |
| 9 | | 77.6 | | 77.7 |
| 10 | 3.16 d, (2.9) | 57.2 | 3.16, d (2.7) | 57.2 |
| 11 | 2.02, dt (11.0, 6.7) | 37.4 | 2.03, m | 37.4 |
| 12$\beta$ | 1.57, dd (11.0, 14.8) | 33.0 | 1.57, dd (11.0, 15.0) | 33.1 |
| 12$\alpha$ | 2.13, dd (6.7, 14.8) | | 2.14, dd (7.0, 15.0) | |
| 13 | | 65.1 | | 65.2 |
| 14 | 1.12, d (5.8) | 31.5 | 1.16, d (5.7) | 31.5 |
| 15 | | 28.3 | | 28.3 |
| 16 | 4.05, d (11.4) | 70.2 | 4.14, d (11.4) | 70.5 |
| | 3.85, d (11.4) | | 3.84, d (11,4) | |
| 17 | 1.13, s | 11.7 | 1.14, s | 11.8 |
| 18 | 0.84, d (6.7) | 18.9 | 0.89, d (6,6) | 18.9 |
| 19 | 1.73, dd (2.9, 1.4) | 10.2 | 1.74, d (2.7, 0.7) | 10.2 |
| 20 | 3.93, d (12,9) | 68.2 | 3.94, d (12,9) | 68.3 |
| | 3.87, d (12,9) | | 3.84, d (12,9) | |
| 1′ | | 178.6 | | 169.5 |
| 2′ | 2.53, sp (7.0) | 35.2 | | 129.7 |
| 3′ | 1.15, d (7.0) | 19.4 | 1.82, s | 12.2 |
| 4′ | 1.14, d (7.0) | 31.6 | 6.84, q (6.8) | 138.8 |
| 5′ | | | 1.81, d superimposed with $H_3$-4″ | 14.4 |
| 1″ | | 175.23 | | 175.1 |
| 2″ | 3.63, s | 42.3 | 3.62, s | 42.4 |
| 3″ | | 134.9 | | 134.9 |
| 4″ | 7.26−7.23, m | 130.4 | 7.24−7.19, m | 129.6 |
| 5″ | 7.31−7.29, m | 129.7 | 7.32−7.28, m | 130.4 |
| 6″ | 7.26−7.23, m | 128.3 | 7.24−7.19, m | 128.2 |

[a]$^1$H NMR (600 MHz, $CD_3OD$). [b]$^{13}$C NMR (151 MHz, $CD_3OD$). [c]$^1$H NMR (500 MHz, $CD_3OD$). [d]$^{13}$C NMR (126 MHz, $CD_3OD$).

concentration of **4**, **7**, and **9** significantly reduced this ratio by 25%, whereas other compounds, such as **2** (see Supporting Information, Movie 4) and **8**, exerted a moderate effect on this ratio (15% reduction) and compound **5** (see Supporting Information, Movie 5) barely reduced this ratio.

These results indicated that, except for phorbol (**1**) and compound **5**, the synthetic and naturally occurring compounds tested were able to facilitate TGF$\alpha$ release. Therefore, for these compounds to exert their effect, the hydroxyl groups at C-12 and C-13 or at C-13 and C-16 need to be esterified. Higher activities were observed when phenylacetate and isobutyrate esters were present, with the most active compound (**3**) bearing two isobutyrate chains. The analysis of TGF$\alpha$ release for compounds isolated from *E. resinifera*, where position C-12 was unsubstituted and positions C-13 and C-16 were acylated, was consistent with this hypothesis. As shown in Figure 3B,C, the effect of compounds **10** (see Supporting Information, Movie 6) and **11** on TGF$\alpha$ release was similar to that of compounds **2** and **8**. All these results agree with the reported effect of DPB, stimulating the release of TGF$\alpha$, in a classical PKC-dependent manner.[10]

**Effect of Phorbol Diesters and 12-Deoxy-16-hydroxyphorbol 13,16-diesters on NPC Proliferation *In Vitro*.** In order to analyze whether the capacity of these compounds to release TGF$\alpha$ correlated with their proliferative activity on NPC, we tested the effect of phorbol (**1**) (as a negative control), compound **5** (no activity on the TGF$\alpha$ assay), compound **2** (mild effect), and compound **3** (most potent on the TGF$\alpha$ assay). In addition, we chose compound **10** as the representative of 12-deoxy-16-hydroxyphorbol 13,16-diesters. We cultured NPCs isolated from the SVZ and cultured them under floating conditions in which the NPCs proliferate and form neurospheres. Cells were left in the absence and presence of increasing concentrations of the different compounds for 48 h. The size of the neurospheres formed was quantified afterward.

We observed no effect in cultures treated with either phorbol (**1**) or compound **5** (these two had shown no effect on TGF$\alpha$ release) (Figure 4A,B). However, all compounds that facilitated TGF$\alpha$ release, independently of their potency in the previous assay (compound **3** showed a stronger effect compared with **2** and **10**), were able to promote NPC proliferation *in vitro*.

This indicated that the amount of TGF$\alpha$ produced by compounds **3**, **2**, and **10** is higher than that required for these cells to proliferate. Interestingly, differences among these compounds are mainly based on the dose−response curve. Thus, compounds **3** and **10** showed different dose−response curves with respect to compound **2** (Figure 4A,B). The first two showed a bell-shaped dose−response curve, whereas the latter showed a linear dose response curve, within the concentration range explored. Maximum effect with **3** and **10** was obtained with nanomolar concentrations, whereas no effect of compound **2** was observed unless a concentration of 5 $\mu$M was used. These results indicated that all compounds with a capacity to facilitate TGF$\alpha$ release were able to promote the proliferation of NPC *in vitro*. However, differences were found in the doses required to exert its proliferative effect, with compounds **3** and **10** being more potent than **2** and also more potent than DPB.[10]

The bell-shaped curve observed for compounds **3** and **10** may be explained by their mechanism of action. As shown in Figure 3C, these compounds stimulate the release of the EGFR ligand TGF$\alpha$. Previous reports have elucidated that the PKC$\alpha$-mediated release of TGF$\alpha$ induced by DPB activates the receptor and its downstream signaling cascades, thus inducing proliferation[10] activating the receptor. However, another role for PKC$\alpha$ is mediated by its capacity to phosphorylate EGFR causing its feedback inhibition.[26] Thus, it is likely that higher doses of compounds **3** and **10** result in the potent inhibition of EGFR and therefore in a reduction of proliferation and neurosphere size.

**Effect of Intranasal Administration of Compounds 2 and 3 on Adult Mouse Neurogenesis in the SVZ.** In order to elucidate whether compounds with the high activity *in vitro* were able to stimulate neurogenesis *in vivo* in the adult mouse brain, compounds **2** (moderate effect in TGF$\alpha$ and neurosphere assays) and **3** (effect at lower concentrations in the neurosphere assay) were administered intranasally during 3


https://doi.org/10.1021/acs.jmedchem.1c00156
J. Med. Chem. 2021, 64, 6070−6084

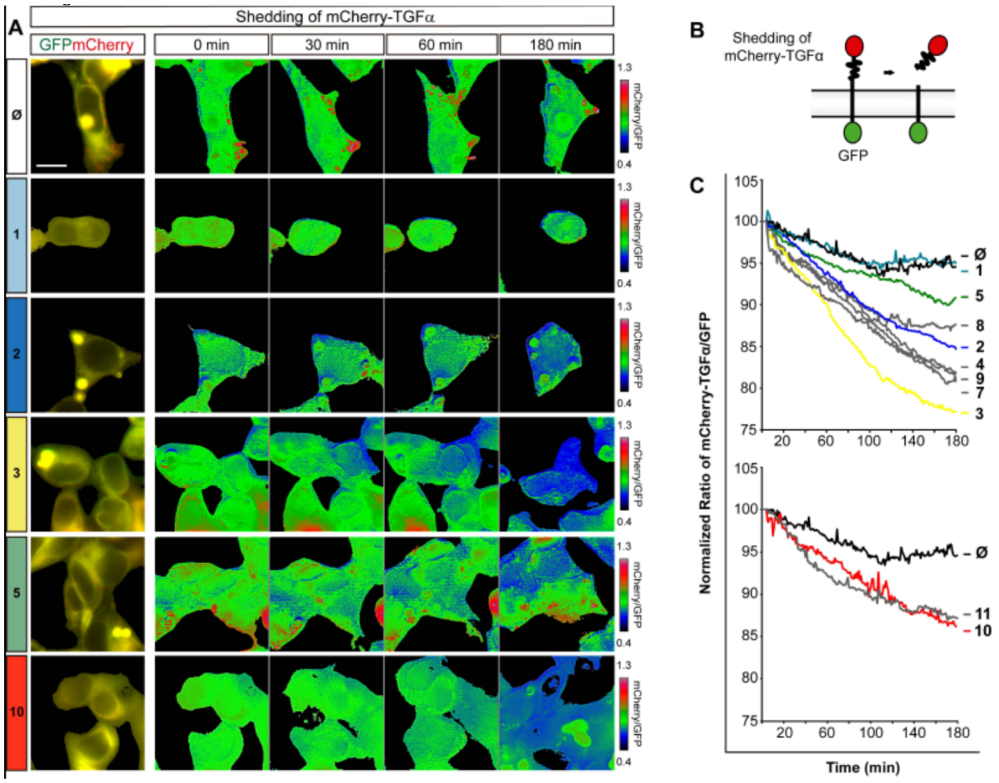


**Figure 3.** Phorbol diesters and 12-deoxy-16-hydroxyphorbol 13,16-diesters can induce mCherry-TGF$\alpha$-GFP ectodomain shedding *in vitro*. (A) Images of mCherry-TGF$\alpha$-GFP expressing, serum-starved HEK293T cells stimulated with diluent, with **1**, **2**, **3**, **5**, or **10** during 180 min. mCherry/GFP ratio images at the indicated time points are shown in the intensity-modulated display mode. The color ranging goes from red to blue to represent mCherry/GFP ratios. The upper and lower limits of the ratio range are shown on the right. Scale bar = 20 $\mu$m. (B) Scheme of mCherry-TGF$\alpha$-GFP construct and its action mechanism. (C) Quantitative analysis of the microscopic images obtained from the time-lapse assays of HEK293T cells expressing mCherry-TGF$\alpha$-GFP protein fusion. mCherry/GFP ratios were normalized to the average mCherry/GFP ratio measured before stimulation with phorbol diesters and 12-deoxy-16-hydroxyphorbol 13,16-diesters. The mean normalized mCherry/GFP ratios are shown, $n$ = 40. All compounds were tested at 0.5 $\mu$M. Ø: none, **1**: phorbol (P), **2**: phorbol 12,13-diacetate, **3**: phorbol 12,13-diisobutyrate, **4**: phorbol 12,13-diphenylacetate, **5**: phorbol 13-isobutyrate, **7**: phorbol 13-isobutyrate-12-phenylacetate, **8**: phorbol 13-isobutyrate-12-tigliate, **9**: phorbol 12-isobutyrate-13-phenylacetate, **10**: DPPI, and **11**: DPPT.

consecutive days. During the 3 days, the mice received injections of the thymidine analogue BrdU to label cells that proliferated during the duration of the treatment. Thereafter, the mice were sacrificed, their brains were sectioned, and immunohistochemistry was performed in the sections containing the SVZ to detect BrdU and the marker of newly generated neuronal progenitors doublecortin (DCX). As shown in Figure 5, and agreeing with the reported effects of DPB,[10] both compounds increased the number of proliferating cells (BrdU +) and the number of proliferative neuronal progenitors (BrdU +/DCX+). However, only compound **3** increased the total DCX cells (DCX burden). Interestingly, the effect of compound **3** on neurogenesis was observed when the concentration of the solution administered daily (12 $\mu$L/day) was 10 nM, whereas no effect was observed when the concentration was 100 nM (10× higher) (Supporting Information, Figure S38) or 5 $\mu$M (data not shown). Thus, for compound **3**, a daily dose of 12 $\mu$L of 10 nM solution had to be used in order to observe an *in vivo* effect. These findings are not surprising, considering the dose−response effect observed *in vitro* in which this compound showed a bell-shaped dose−response curve with the maximum activity at 50 nM and a decline when higher doses of the compound were used. Although the actual concentrations used *in vitro* and *in vivo* should not be compared because the concentration of this compound in the SVZ or DG after the 3-day treatment period is not known, it is reasonable to suggest that the *in vitro* dose response curve and the *in vivo* effect on neurogenesis agree. The reason for the lack of activity at high doses of compound **3** can be explained by its mechanism of action. As explained above, the reported effect of DPB on adult hippocampal neurogenesis was mediated by its capacity to activate PKC$\alpha$[10] inducing TGF$\alpha$ release and EGFR activation. Thus, it is reasonable to suggest that the mechanism of action of compound **3** is similar and results in the activation of EGFR as well. In light of the results shown herein, it is evident that low concentrations of **3** are enough to release the amount of TGF$\alpha$ required to saturate the EFGR receptor and initiated the EGFR-associated signaling pathways that promote proliferation. In this context, the lack of effect at high doses might be explained if elevated doses of the compound over-activate PKC$\alpha$ and directly phosphorylate EGFR, mediating the feedback inhibition of the receptor.[26]

**Physicochemical Properties and SAR Analysis.** To investigate the influence of an additional ester group, we compared the previous results obtained with 12-deoxyphorbols[9,10] with those described herein. Thus, in comparison to prostratin, the introduction of an additional acetyloxy moiety leads to an increased proliferative effect in compound **2** (phorbol 12,13-diacetate). A similar effect was observed when


https://doi.org/10.1021/acs.jmedchem.1c00156
J. Med. Chem. 2021, 64, 6070−6084

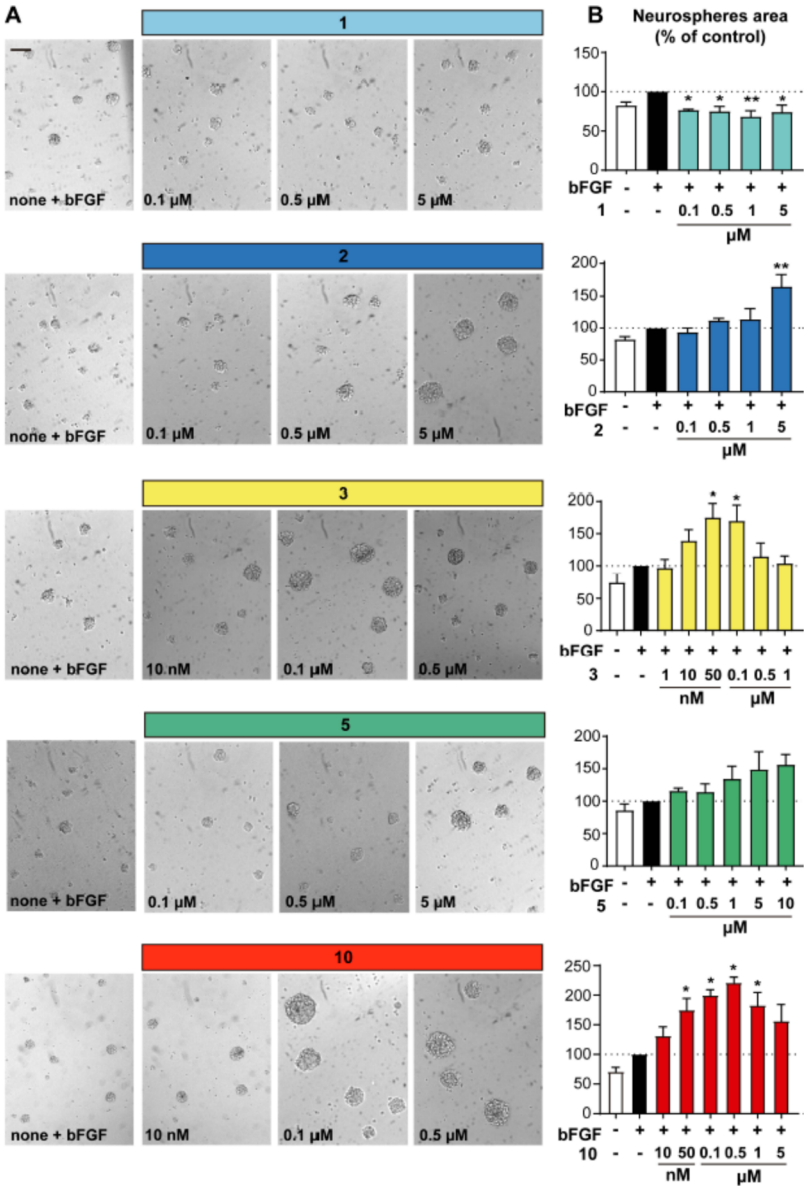


**Figure 4.** Effect of phorbol diesters and 12-deoxy-16-hydroxyphorbol 13,16-diesters on NPC proliferation *in vitro*. (A) Representative phase-contrast microscopy images of neurospheres cultured for 72 h in the presence of **1**, **2**, **3**, **5**, and **10**. Scale bar = 100 $\mu$m. (B) Graph shows the effect of the different treatments at different concentrations on the neurosphere area expressed as the percentage of control (only bFGF treatment). Data shown are the mean ± SEM of nine independent measurements. Statistical analysis: ***$p < 0.0001$ in two-tailed unpaired Student's *t*-test comparing bFGF with bFGF + treatment. **1**: phorbol, **2**: phorbol 12,13-diacetate, **3**: phorbol 12,13-diisobutyrate, **5**: phorbol 13-isobutyrate, and **10**: DPPI.

comparing DPB with phorbol 12,13-diisobutyrate (**3**) and DPP with 12-deoxy-16-hydroxyphorbol 16-isobutyrate-13-phenyl acetate (**10**).

Two additional factors directly influence the effect of the compound described in this work on NPC expansion: the nature and location of side chains on the tigliane skeleton.

Comparing compounds with the same substituent located in different positions (**9** *vs* **10** or **7** *vs* **9**), it is observed that changing a substituent from C-12 to C-16 produces a significant reduction in the proliferative effect; however, no difference is observed when substituents are exchanged between C-12 and C-13. Remarkably, while the modification of the chain at C-12 in compounds bearing a phenylacetyl group at C-13 does not produce changes in the activity (compare compounds **4** and **9**, Figure 3C), significant differences were observed when the group located at C-13 is an isobutyrate (compare compounds **3**, **7**, and **8**, Figure 3C).

Table S1 (Supporting Information) summarizes physicochemical parameters of the tested compounds, including molecular lipophilicity (log *P*), bulkiness (MW), H-bond features (HBA, HBD, and topological polar surface area (TPSA)), and molar refractivity. All of them possess a greater number of H-bond acceptors (HBA = 6−8) than H-bond donors (HBD = 3−5); only those with HBD > 3 (compounds **1** and **5**) proved to show no activity. On the other hand, the previously reported and active 12-deoxyphorbol esters[9,10] possess HBD = 3 (Supporting Information, Table S2), which is consistent with the analysis shown above, suggesting that the number of HBD seem to be essential for activity.


https://doi.org/10.1021/acs.jmedchem.1c00156
J. Med. Chem. 2021, 64, 6070−6084

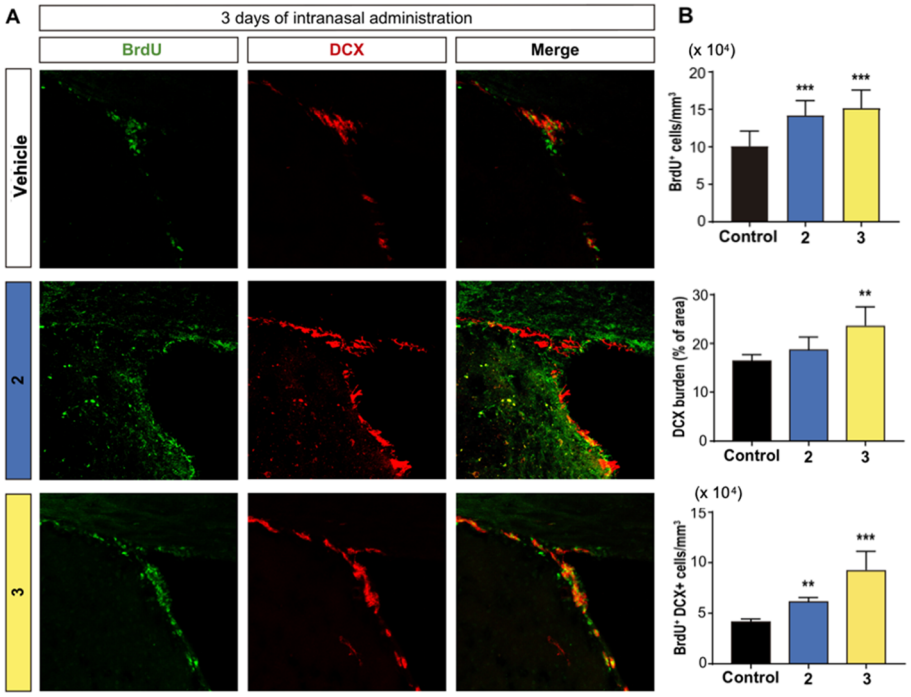


**Figure 5.** Effect of the intranasal administration of phorbol diesters on BrdU+ and DCX + cells in the SVZ *in vivo*. Intranasal administration of **2** (5 $\mu$M), **3** (10 nM), or only the vehicle was performed during 3 days to healthy 2 month-old adult mice. All mice were intraperitoneally injected with BrdU (100 mg/kg) on the last day of treatment as described in methods. (A) Representative confocal microscopy images of the SVZ of adult mice treated with **2**, **3**, or only the vehicle. Slides were processed for the immunohistochemical detection of the proliferation marker BrdU and DCX. Scale bar = 50 $\mu$m. (B) Graph shows the number of proliferating cells marked with BrdU per mm,[3] the percentage of DCX burden, and the number of BrdU + cells per mm$^3$ that co-expressed DCX marker in the SVZ. Data shown are the mean ± SEM; $n$ = 6 animals per group. Statistical analysis: *$p$ < 0.05 by Student's $t$-test comparing with the control group. **2**: phorbol 12,13-diacetate and **3**: phorbol 12,13-diisobutyrate.

**Docking Analysis of Phorbol Derivatives with PKC$\delta$C1B (PDB: 1PTR) and PKC$\beta$C1B (PDB: 3PFQ).** PKC activation is delicately controlled by several factors, involving its conformational change and membrane translocation. Phorbol esters show a higher affinity for the C-1 domain than the natural substrate (diacylglycerol, DAG), which, in part, explains their ability to promote PKC activation. Phorbol esters bind to the hydrophilic cleft of C-1 through hydrogen bonding interactions, which may result in a hydrophobic capping of the C-1 domain, depending on the nature of the substituents at C-12 and C-13 in the phorbol ester.[27] The phorbol ester/PKC complex can now eventually translocate to the membrane, which has been described as part of the activation process.

A right balance in the lipophilicity of the substituents of the phorbol esters would translate into a balanced activation of PKC.[28] The crystal structure (PDB ID: 1PTR)[27] of PKC$\delta$C1B complexed with phorbol 13-acetate describes the binding pocket as a V-shape, surrounded by two long $\beta$-sheets. The PKC$\delta$C1B binds to phorbol 13-acetate through three residues: Gly-253, Thr-242, and Leu-251. Such residues target phorbol 13-acetate in specific atoms, where they made three hydrogen bonds with the hydroxyl group in position C-20 and another two with both oxygens in positions C-3 and C-4.[29] Transformation of any groups located at these positions would affect the ligand-binding affinity. On the other hand, phorbol esters' ability to bind PKC isoforms depends on the structural characteristics of the C-1 domains in each one.[29] Previous results have shown that the capacity to promote proliferation of NPC is related to their ability to activate classical PKC.[10,30] Therefore, to further understand the structure−activity relationship, selected phorbol esters (**1**, **3**, and **7**), 12-deoxyphorbol esters (DPB and DPA), and 12-deoxy-16-hydroxyphorbol esters (**10** and **11**) were subjected to *in silico* molecular docking with C-1 domain models of a classical PKC. Previously, due to the availability of the crystal structure of the PKC$\delta$C1B/phorbol 13-acetate complex, we investigated possible interactions of the acyl groups at C-13, C-12/C-13, and C-13/C-16 with residues on the walls of the receptor groove PKC$\delta$. Then, we extended our analysis such that we were able to identify key determinants of the interaction of phorbol esters with the C1 domain of PKC$\beta$, involved in the promotion of NPC proliferation.[10,30] The subdomain C1 of PKC$\beta$ was determined from the full-length proteins PKC$\beta$II (PDB ID: 3PFQ).[31] The activator-binding residues of PKC$\beta$ were identified by comparison with the activator-binding residues of PKC$\delta$-C1B (sequence homology was 62%, Figure 6).

Despite differences in some residues, alignment of the crystal structures of $\delta$C1B (blue) and $\beta$C1B (gray) has shown a remarkable similarity in the activation of binding residues, including GLY-253 $\delta$C1B/GLY-124 $\beta$C1B, LEU-251 $\delta$C1B/LEU-122 $\beta$C1B, and THR-242 $\delta$C1B/THR-113 $\beta$C1B). The differences between $\delta$C1B and $\beta$C1B were in the following residues Met-239 $\delta$C1B → Ser-110 $\beta$C1B, Trp-252 $\delta$C1B → Tyr-123 $\beta$C1B, Val-255 $\delta$C1B → Ile-126 $\beta$C1B, and Lys-256 $\delta$C1B → His-127 $\beta$C1B.

Identical hydrogen bond interactions to those previously described for phorbol 13-acetate[29] were observed in all compounds except in phorbol (**1**), which showed an extra interaction between the hydroxyl group in C-13 and Ser110 of PKC $\beta$ (equivalent to Met239 of PKC$\delta$) (Supporting


https://doi.org/10.1021/acs.jmedchem.1c00156
J. Med. Chem. 2021, 64, 6070−6084

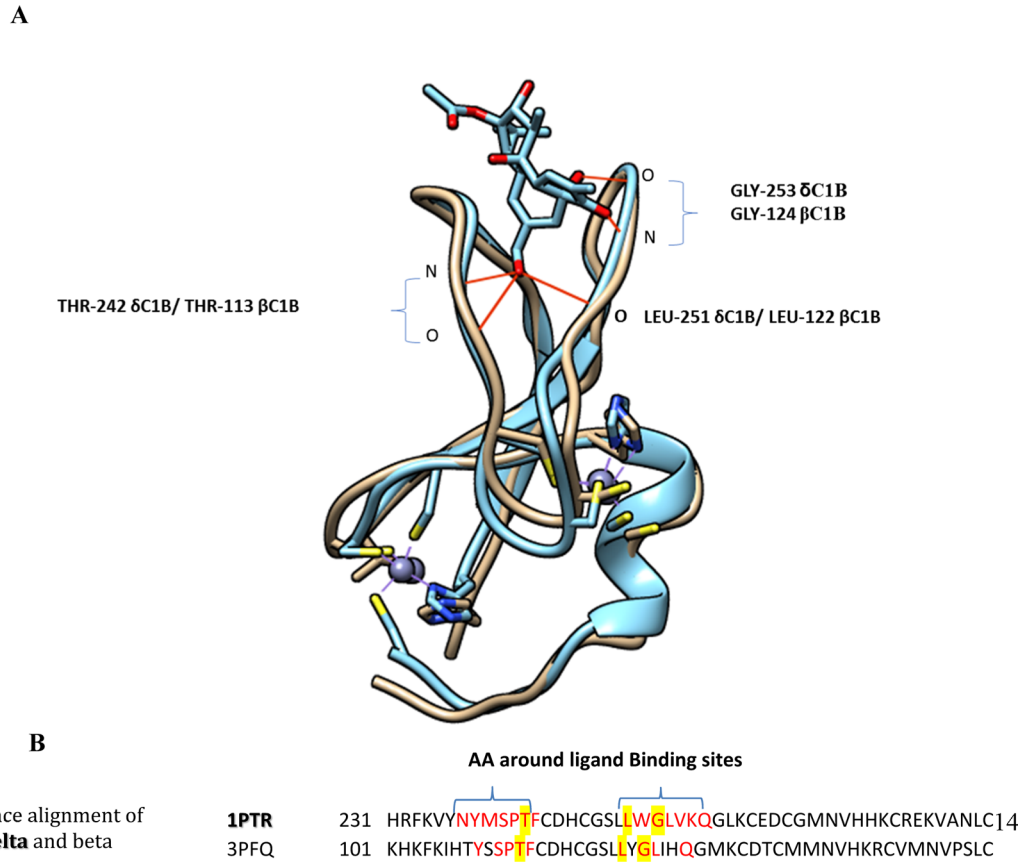


**Figure 6.** (A) Structural and sequence comparison of the zinc finger of PKC$\delta$C1B (blue) and PKC$\beta$C1B (gray). *In silico* interaction with phorbol 13-acetate is included for comparison with the crystal structure (PDB ID: 1PTR) of PKC$\delta$C1B complexed with phorbol 13-acetate. (B) Sequence alignment of PKC$\delta$C1B and PKC$\beta$II-C1B (amino acids (AA) in red are the AA around the ligand-binding site, and the AA marked in yellow are the AA that form hydrogen bonds with phorbol esters).

Information, Figures S39 and S40). No differences were observed in the way in which the C-12, C-13-diester and C-13, C-16-diester were located inside the pocket, confirming that hydrogen bond interactions between oxygenated functions on A and B rings ($C_3O$, $C_4OH$, and $C_{20}OH$ and Gly-124, Thr-113, and Leu-122 of PKC$\beta$, equivalent to Gly-253, Thr-242, and Leu-251 of PKC$\delta$) are the factors that determine how these compounds bind the C-1 domain of PKC.

Experimentally, neurosphere assays have shown that 12-deoxyphorbols (DPP and DPB)[9] are weaker promoters of NPC proliferation than DPPI (**10**) and phorbol ester **3** (Figure 4), confirming that the presence of an extra ester function (either at C-12 or at C-16) favors an activity increase. On the other hand, TGF$\alpha$ assays, which we have shown to correlate with the promotion of NPC proliferation, show that phorbol 12,13-diesters **3** and **7** are more potent than 12-deoxy-16-hydroxyphorbol 13,16-diesters **10** and **11**, the difference between them being the disposition inside (**10** and **11**) or outside (**3**, **7**) of the C-1-domain receptor gap of the extra ester function, either at C-12 or at C-16, respectively (Supporting Information, Figure S40). This indicates that the additional side chains present on these compounds are key factors for activity, which would be consistent with an increase of the interaction of the phorbol ester/PKC complex with the membrane and a better modulation of the PKC activity.

## CONCLUSIONS

In summary, we describe the preparation of a small library of phorbol 12,13-diesters, which were also used in a targeted UHPLC−HRMS screening of the latex of *E. resinifera*. This approach led to the identification and isolation of two new 12-deoxy-16-hydroxyphorbol 13,16-diesters. The ability of these compounds to induce TFG$\alpha$, to increase NPC proliferation, and to stimulate neurogenesis was evaluated. All compounds that facilitated TGF$\alpha$ release were able to promote NPC proliferation when evaluated *in vitro*.

The presence of an extra acyloxy moiety at the C or D rings of the tigliane skeleton leads to an increased level of activity compared with equivalent 12-deoxyphorbol 13-esters, which decreases if a free hydroxyl group is at C-12. While the number of hydrogen bond donors appears to be a determinant factor for activity, this is modulated by additional side-chain interactions.

Remarkably, compound **3**, bearing isobutyryloxy groups at C-12 and C-13, was the most potent compound on the TGF$\alpha$ assay and in the *in vitro* NPC proliferation assay, also leading to neurogenesis *in vivo* when administered intranasally to mice.

Considering the effect of similar compounds like DPB at improving episodic memory in mice,[10] these results point out at phorbol diesters, like those described here, as relatively simple-to-manufacture pharmacological agents in the development of treatments for disorders associated with a reduction in neurogenesis and memory impairment such as neurodegenerative diseases.


https://doi.org/10.1021/acs.jmedchem.1c00156
J. Med. Chem. 2021, 64, 6070−6084

## EXPERIMENTAL SECTION

**General.** Silica gel (Merck, grade 60, particle size 0.04−0.063 mm, 230−240 mesh ASTM) was used for column chromatography. TLC was performed on Merck Kiesegel 60 F254, 0.25 mm thick. Optical rotations were determined with a Jasco P-2000 digital polarimeter. Infrared spectra were recorded on a PerkinElmer Spectrum BX FT-IR spectrophotometer and reported as wavenumber ($cm^{-1}$). $^1H$ and $^{13}C$ NMR measurements were recorded on Agilent 400, 500, and 600 MHz NMR spectrometers. Chemical shifts are expressed in ppm ($\delta$) referenced to the solvent used, and $J$ values are reported in Hz. The multiplicity of the signals (s, singlet; d, doublet; dd, doublet of doublets; t, triplet; td, triplet of doublets; q, quadruplet; qt, quintuplet; hept, heptuplet; and m, multiplet), the coupling constants ($J$), and the specific characterization of each compound are shown. Spectra were assigned using appropriate COSY, DEPT, HSQC, HMBC, and NOESY sequences. HRMS was performed in a Waters Xevo G2-S QTof mass spectrometer in the positive-ion or negative-ion ESI mode. HPLC purification was performed with a Merck-Hitachi LaChrom apparatus equipped with an UV−vis detector (L 4250), a differential refractometer detector (RI-7490), and an Elite LaChrom-Hitachi apparatus equipped with a differential refractometer detector (RI-2490). LiChroCART LiChrospher Si 60 (5 $\mu$m, 250 mm × 4 mm) and LiChroCART LiChrospher Si 60 (10 $\mu$m, 250 mm × 10 mm) columns were used for isolation experiments. The purity of the tested compounds was determined by HPLC−UV with a Hitachi Primaide or by HPLC−RI with a Hitachi Chromaster HPLC systems. The purity of all tested compounds is >95%.

**UHPLC−HRMS Conditions.** The analyses were run on a separation system, ACQUITY UPLC H-Class system, with a binary solvent system and an automatic sample manager that was equipped with an UPLC BEH C18 (2.1 mm × 100 mm, 1.7 mm) column, running at a temperature of 55 °C. The mobile phases consisted of eluent A (0.1% formic acid in water, v/v) and eluent B (methanol). These phases were delivered at a flow rate of 0.3 mL/min by using a linear gradient program as follows: 0−0.5 min, 25% A; 0.5−5 min, 25−0% A; 5−7 min, 0% A; 7−8 min, 0−25% A; and 8−10 min, 25% A. The injection volume of all samples was 2 mL.

The UHPLC system was coupled with a quadrupole time-of-flight tandem mass spectrometer (Xevo-G2-S QTOF; Waters, Manchester, U.K.) equipped with an ESI source. The operating parameters in ESI and the data-independent acquisition mode ($MS^E$)[23] were set as follows in positive and negative modes: sample cone voltage of 30 V; source temperature of 120 °C; cone gas flow of 10 L/h; and desolvation gas flow of 850 L/h. In the positive mode, capillary voltage and desolvation temperature were set at 0.7 kV and 400 °C, respectively. In the negative mode, capillary voltage and desolvation temperature were set at 3.0 kV and 450 °C, respectively. In the $MS^E$ mode (positive mode), the trap collision energy of the low-energy function was set at 6 eV, while the ramp trap collision energy of the high-energy function was set at 60−120 eV.

To ensure mass accuracy and reproducibility, the mass spectrometer was calibrated over a range of 100−1200 Da using sodium formiate solution. Leucine-enkephalin ($m/z$ 556.2771 in positive-ion mode) was used as the external reference of LockSpray infused at a constant flow of 20 mL/min. Data acquisition was performed by MassLynx 4.1 software (Waters, Manchester, U.K.) in positive and negative-ion modes.

**Synthesis of Phorbol Esters.** *Preparation of Phorbol 12,13-Diacetate-20-trityl (**2a**).* Pyridine (2 drops) was added to a solution of phorbol-20-trityl (**1a**) (60.0 mg, 0.1 mmol) in acetic anhydride (2 mL) and stirred at room temperature overnight. Then, cyclohexane was added (5 mL), and the solvent was evaporated under reduced pressure. This procedure was repeated three times to give quantitatively phorbol-12,13-diacetate-20-trityl (**2a**) (67.6 mg, 99%). Spectroscopic data of compound **2a** were identical to those described in the literature.[20]

*General Procedure for the Preparation of 12,13-Diacylphorbols **3a** and **4a**.* A mixture of phorbol-20-trityl (**1a**) (0.13 mmol), the corresponding isobutyric acid or phenylacetic acid (1.13 mmol), and DMAP (0.13 mmol) in dry $CH_2Cl_2$ (2 mL) was stirred for 10 min. To the resulting mixture was added EDCI (1.13 mmol). After stirring for 18 h, the reaction mixture was evaporated, and then $Et_2O$ (5 mL) was added. The crude was sequentially washed with $H_2O$ (5 mL), twice with saturated sodium bicarbonate solution (5 mL), and $H_2O$ (2 mL), dried over anhydrous sodium sulfate, filtered, and evaporated under reduced pressure to afford compounds **3a** and **4a**.

*Phorbol 12,13-Diisobutyrate-20-trityl (**3a**) (99%).* White amorphous powder; $[\alpha]_D^{21}$ + 50.9 ($c$ 2.0, $CH_3OH$). IR (KBr) $\upsilon_{máx}$: 3408, 3059, 2975, 2934, 1735, 1714, 1469, 1369, 1194, 1156, 1076, 980, and 758 $cm^{-1}$. $^1H$ NMR ($CD_3OD$, 500 MHz) $\delta$: 7.56 (m, 1H), 7.41−7.38 (m, 6H), 7.30−7.26 (m, 6H), 7.24−7.20 (m, 3H), 5.56 (d, $J$ = 5.8 Hz, 1H), 5.42 (d, $J$ = 10.1 Hz, 1H), 3.57 (d, $J$ = 11.1 Hz, 1H), 3.49 (d, $J$ = 11.1 Hz, 1H), 3.19 (m, 2H), 2.61−2.52 (m, 2H), 2.50 (br s, 2H), 2.23 (dq, $J$ = 10.1, 6.6 Hz, 1H), 1.75 (dd, $J$ = 2.7, 1.4 Hz, 3H), 1.28 (s, 3H), 1.23 (s, 3H), 1.19−1.15 (m, 12H), 1.08 (d, $J$ = 5.1 Hz, 1H), and 1.38 (d, $J$ = 6.6 Hz, 3H). $^{13}C$ NMR ($CD_3OD$, 125 MHz) $\delta$: 210.2, 180.8, 178.5, 160.4, 145.5 (3C), 140.7, 134.4, 130.8, 129.8 (6C), 128.8 (6C), 128.1 (3C), 88.2, 79.5, 78.1, 74.9, 69.9, 66.8, 57.4, 44.3, 40.4, 38.9, 37.0, 35.5, 27.3, 24.2, 19.5, 19.2, 19.0, 18.9, 17.4, 14.7, and 10.2. HRMS (ESI): $m/z$ calcd for $C_{47}H_{54}O_8Na$ $[M + Na]^+$, 769.3716; found, 769.3712.

*Phorbol 12,13-Diphenylacetate-20-trityl (**4a**) (82%).* Spectroscopic data of compound **4a** were identical to those described in the literature.[32]

*General Procedure for Monoacylation at C-13. Preparation of Compounds **5a** and **6a**.* A mixture of phorbol-20-trityl ether (**1a**) (0.13 mmol), the corresponding isobutyric acid or phenylacetic acid (0.4 mmol), and DMAP (0.03 mmol) in dry $CH_2Cl_2$ (2 mL) was stirred for 10 min. To the resulting mixture was added EDCI (0.4 mmol). After stirring for 2 h, the reaction mixture was evaporated and then $Et_2O$ (5 mL) was added. The crude was sequentially washed with $H_2O$ (5 mL), twice with saturated sodium bicarbonate solution (5 mL), and $H_2O$ (2 mL), dried over anhydrous sodium sulfate, filtered, and evaporated under reduced pressure to afford compounds **5a** and **6a**.

*Phorbol 13-Isobutyrate-20-trityl (**5a**) (99%).* White amorphous powder; $[\alpha]_D^{21}$ + 38,08 ($c$ 4.7, $CH_3OH$). IR (KBr) $\upsilon_{máx}$: 3411, 3059, 2977, 2927, 2877, 1710, 1448, 1324, 1204, 1159, 1048, 992, 758, and 706 $cm^{-1}$. $^1H$ NMR ($CD_3OD$, 500 MHz) $\delta$: 7.58 (m, 1H), 7.41−7.38 (m, 6H), 7.29−7.25 (m, 6H), 7.23−7.19 (m, 3H), 5.54 (d, $J$ = 5.9 Hz, 1H), 3.87 (d, $J$ = 9.7 Hz, 1H), 3.56 (d, $J$ = 11.0 Hz, 1H), 3.49 (d, $J$ = 11.0 Hz, 1H), 3.15 (m, 2H), 2.63 (hept, $J$ = 7.0 Hz, 1H), 2.49 (s, 2H), 2.04 (dq, $J$ = 9.7, 6.71H), 1.76 (dd, $J$ = 3.0, 1.3 Hz, 3H), 1.24 (s, 6H), 1.19 (d, $J$ = 7.0 Hz, 6H), 1.07 (d, $J$ = 6.5 Hz, 3H), and 0.98 (d, $J$ = 5.3 Hz, 1H). $^{13}C$ NMR ($CD_3OD$, 125 MHz) $\delta$: 210.5, 181.6, 160.9, 145.5 (3C), 140.3, 134.2, 131.3, 129.8 (6C), 128.8 (6C), 128.1 (3C), 88.1, 79.4, 77.5, 74.9, 70.0, 69.0, 57.7, 46.2, 40.4, 39.0, 36.6, 35.5, 27.1, 24.3, 19.2, 19.1, 17.4, 15.4, and 10.3. HRMS (ESI): $m/z$ calcd for $C_{43}H_{48}O_7Na$ $[M + Na]^+$, 699.3298; found, 699.3297.

*Phorbol 13-Phenylacetate-20-trityl (**6a**) (67%).* Spectroscopic data of compound **6a** were identical to those described in the literature.[33]

*General Procedure for the Preparation of 12,13-Diacylphorbols **7a**−**9a**.* Phorbols **7a** and **8a** were prepared from **5a** and phorbol **9a** from **6a** following the procedure described above for the synthesis of **3a** and **4a**.

*Phorbol 12-Phenylacetate-13-isobutyrate-20-trityl (**7a**) (73%).* White amorphous powder; $[\alpha]_D^{21}$ 26.3 ($c$ 3.1, $CH_3OH$). IR (KBr) $\upsilon_{máx}$: 3330, 3059, 3022, 2972, 2917, 2872, 1706, 1447, 1348, 1251, 1157, 1049, 980, and 702 $cm^{-1}$. $^1H$ NMR ($CD_3OD$, 500 MHz) $\delta$: 7.53 (m, 1H), 7.38−7.17 (m, 20H), 5.52 (d, $J$ = 5.8 Hz, 1H), 5.40 (d, $J$ = 10.5 Hz, 1H), 3.68−3.61 (m, 2H), 3.54 (d, $J$ = 11.2 Hz, 1H), 3.47 (d, $J$ = 11.2 Hz, 1H), 3.16 (t, $J$ = 2.5 Hz, 1H), 3.12 (t, $J$ = 5.8 Hz, 1H), 2.52 (m, 1H), 2.48 (br s, 2H), 2.18 (dq, $J$ = 10.5, 6.5 Hz,1H), 1.73 (dd, $J$ = 2.4, 1.5 Hz, 3H), 1.12 (d, $J$ = 7.0 Hz, 6H), 1.08 (s, 3H), 1.05 (s, 3H), 1.00 (d, $J$ = 5.1 Hz, 1H), and 0.84 (d, $J$ = 6.5 Hz, 3H). $^{13}C$ NMR ($CD_3OD$, 125 MHz) $\delta$: 210.2, 180.7, 173.3, 160.3, 145.5 (3C), 140.6, 135.8, 134.4, 130.7, 130.2 (2C), 129.8 (6C), 129.6 (2C), 128.8 (6C), 128, 1 (4C), 88.1, 79.4, 78.7, 74.8, 69.9, 66.6, 57.3, 44.1, 42.5, 40.3, 38.8, 37.0, 35.5, 27.3, 24.0, 19.0, 18.9, 17.0, 14.7, and 10.3.


https://doi.org/10.1021/acs.jmedchem.1c00156
J. Med. Chem. 2021, 64, 6070−6084

HRMS (ESI): $m/z$ calcd for $C_{51}H_{54}O_8Na$ $[M + Na]^+$, 817.3716; found, 817.3730.

*Phorbol 12-Tigliate-13-isobutyrate-20-trityl (**8a**) (47%).* White amorphous powder; $[\alpha]_D^{21}$ + 17.5 ($c$ 1.25, $CH_3OH$). IR (KBr) $\upsilon_{máx}$: 3402, 2978, 2950, 1712, 1448, 1361, 1254, 1219, 1156, 1082, 770, and 705 $cm^{-1}$. $^1H$ NMR ($CD_3OD$, 400 MHz) $\delta$: 7.56 (m, 1H), 7.41−7.37 (m, 6H), 7.30−7.21 (m, 9H), 6.85 (dq, $J$ = 7.2, 1.4 Hz, 1H), 5.56 (d, $J$ = 6.1 Hz, 1H), 5.48 (d, $J$ = 10.4 Hz, 1H), 3.58 (d, $J$ = 11.1 Hz, 1H), 3.50 (d, $J$ = 11.1 Hz, 1H), 3.20 (m, 2H), 2.57 (hept, $J$ = 7.0 Hz, 1H), 2.51 (s, 2H), 2.27 (dq, $J$ = 10.4, 6.4 Hz, 1H), 1.82 (m, 6H), 1.75 (dd, $J$ = 2.6, 1.4 Hz, 3H), 1.31 (s, 3H), 1.23 (s, 3H), 1.15 (d, $J$ = 7.0 Hz, 6H), 1.08 (d, $J$ = 5.1 Hz, 1H), and 0.87 (d, $J$ = 6.4 Hz, 3H). $^{13}C$ NMR ($CD_3OD$, 100 MHz) $\delta$: 210.0, 180.7, 169.1, 160.2, 145.3 (3C), 140.5, 138.8, 134.2, 130.6, 129.6 (6C), 129.4, 128.6 (6C), 127.9 (3C), 87.9, 79.3, 78.0, 74.7, 69.7, 66.6, 57.1, 44.3, 40.2, 38.7, 36.9, 35.2, 27.1, 23.9, 18.8, 17.3, 14.5, 14.2, 12.1, and 10.0. HRMS (ESI): $m/z$ calcd for $C_{48}H_{54}O_8Na$ $[M + Na]^+$, 781.3716; found, 781.3712.

*Phorbol 12-Isobutyrate-13-phenylacetate-20-trityl (**9a**) (82%).* White amorphous powder; $[\alpha]_D^{21}$ + 28.5 ($c$ 1.5, $CH_3OH$). IR (KBr) $\upsilon_{máx}$: 3414, 2976, 2924, 2878, 1715, 1626, 1469, 1269, 1218, 1154, 759, and 705 $cm^{-1}$. $^1H$ NMR ($CD_3OD$, 500 MHz) $\delta$: 7.54 (m, 1H), 7.39−7.19 (m, 20H), 7.30−7.21 (m, 9H), 5.521 (d, $J$ = 6.3 Hz, 1H), 5.47 (d, $J$ = 10.5 Hz, 1H), 3.67 (s, 2H), 3.56 (d, $J$ = 11.1 Hz, 1H), 3.48 (d, $J$ = 11.1 Hz, 1H), 3.15 (m, 2H), 2.56 (hept, $J$ = 7.0 Hz, 1H), 2.51−2.46 (s, 2H), 2.21 (dq, $J$ = 10.5, 6.5 Hz, 1H), 1.74 (dd, $J$ = 3.0, 1.4 Hz, 3H), 1.24 (s, 3H), 1.16 (d, $J$ = 7.0 Hz, 3H), 1.15 (d, $J$ = 7.0 Hz, 3H), 1.05 (s, 3H), 1.02 (d, $J$ = 5.1 Hz, 1H), and 0.88 (d, $J$ = 6.5 Hz, 3H). $^{13}C$ NMR ($CD_3OD$, 125 MHz) $\delta$: 210.2, 178.6, 175.7, 160.3, 145.5 (3C), 140.7, 134.9, 134.4, 130.7 (2C), 130.6, 129.8 (6C), 129.5 (2C), 128.8 (6C), 128.1, 128.1 (3C), 88.1, 79.5, 78.1, 74.8, 69.8, 67.4, 57.4, 44.3, 42.1, 40.3, 38.8, 36.9, 35.4, 27.5, 24.0, 19.4, 19.2, 17.4, 14.7, and 10.2. HRMS (ESI): $m/z$ calcd for $C_{51}H_{54}O_8Na$ $[M + Na]^+$, 817.3716; found, 817.3707.

*General Procedure for the Deprotection of Trityl Ether. Preparation of Phorbols **2**−**9**.* $HClO_4$ (0.01 M solution in methanol, 1 mL, 0.01 mmol) was added to a solution of the corresponding phorbols **2a**−**9a** (0.05 mmol) in methanol (1 mL). Once the reaction was completed (30 min.), sodium acetate was added until pH = 7. The solvent was evaporated under reduced pressure to give a crude product which was purified by silica gel column chromatography. Elution with petroleum ether/ethyl acetate (50:50) yielded the corresponding compounds **2**−**9**.

*Phorbol 12,13-Diacetate (**2**) (99%).* Spectroscopic data of compound **2** were identical to those described in the literature.[34] Purity HPLC: 99.8%.

*Phorbol 12,13-Diisobutyrate (**3**) (87%).* White amorphous powder; $[\alpha]_D^{21}$ + 19.1 ($c$ 2.2, $CHCl_3$). IR (KBr) $\upsilon_{máx}$: 3405, 2975, 2926, 2878, 1712, 1469, 1389, 1275, 1160, 1080, 978, and 754 $cm^{-1}$. $^1H$ NMR ($CD_3OD$, 500 MHz) $\delta$: 7.54 (m, 1H), 5.61 (d, $J$ = 4.7 Hz, 1H), 5.41 (d, $J$ = 10.3 Hz, 1H), 3.96 (d, $J$ = 13.9 Hz, 1H), 3.91 (d, $J$ = 13.9 Hz, 1H), 3.30 (m, 1H), 3.16 (t, $J$ = 2.7 Hz, 1H), 2.63−2.53 (m, 4H), 2.22 (dq, $J$ = 10.5, 6.3 Hz, 1H), 1.73 (dd, $J$ = 2.7, 1.4 Hz, 3H), 1.27 (s, 3H), 1.21 (s, 3H), 1.19−1.14 (m, 12H), 1.10 (d, $J$ = 5.3 Hz, 1H), and 0.88 (d, $J$ = 6.5 Hz, 3H). $^{13}C$ NMR ($CD_3OD$, 125 MHz) $\delta$: 210.3, 180.7, 178.5, 160.5, 142.9, 134.6, 129.3, 79.8, 78.1, 74.7, 68.0, 66.8, 57.3, 44.3, 40.0, 38.5, 37.3, 35.5 (2C), 27.3, 24.2, 19.4, 19.2, 19.0, 18.9, 17.5, 14.8, and 10.2. Purity HPLC: 96.6%. HRMS (ESI): $m/z$ calcd for $C_{28}H_{39}O_8$ $[M - H]^-$, 503.2645; found, 503.2641.

*Phorbol 12,13-Diphenylacetate (**4**) (90%).* White amorphous powder; $[\alpha]_D^{21}$ + 24.2 ($c$ 7.0, $CHCl_3$). IR (KBr) $\nu_{máx}$: 3415, 2924, 2854, 1710, 1628, 1455, 1330, 1076, 998, and 751 $cm^{-1}$. $^1H$ NMR ($CD_3OD$, 400 MHz) $\delta$: 7.51 (m, 1H), 7.34−7.21 (m, 10H), 5.54 (d, $J$ = 5.6 Hz, 1H), 5.45 (d, $J$ = 10.4 Hz, 1H), 3.92 (d, $J$ = 13.1 Hz, 1H), 3.89 (d, $J$ = 13.1 Hz, 1H), 3.65 (s, 2H), 3.64 (s, 2H), 3.20 (t, $J$ = 5.6 Hz, 1H), 3.11 (t, $J$ = 2.6 Hz, 1H), 2.49 (d, $J$ = 19.0 Hz, 1H), 2.44 (d, $J$ = 19.0 Hz, 1H), 2.14 (dq, $J$ = 10.4, 6.6 Hz, 1H), 1.72 (dd, $J$ = 2.6, 1.4 Hz, 3H), 0.98 (d, $J$ = 5.6 Hz, 1H), 0.96 (s, 3H), 0.88 (s, 3H), and 0.84 (d, $J$ = 6.6 Hz, 3H). $^{13}C$ NMR ($CD_3OD$, 100 MHz) $\delta$: 210.3, 175.7, 173.5, 160.5, 142.8, 135.8, 134.8, 134.6, 130.7 (2C), 130.3 (2C), 129.6 (2C), 129.5 (2C), 129.2, 128.2, 128.1, 79.8, 78.9, 74.7, 67.9, 67.3, 57.3, 44.2, 42.5, 42.2, 39.9, 38.4, 37.1, 27.5, 23.8, 17.0, 14.7, and 10.2. Purity HPLC: 98.1%. HRMS (ESI): $m/z$ calcd for $C_{36}H_{40}O_8Na$ $[M + Na]^+$, 623.2621; found, 623.2616.

*Phorbol 13-Isobutyrate (**5**) (84%).* White amorphous solid; $[\alpha]_D^{21}$ + 48.4 ($c$ 2.0, $CHCl_3$); IR (KBr) $\upsilon_{máx}$: 3414, 2924, 2854, 1638, 1491, 1329, 1291, 1159, 1015, and 792 $cm^{-1}$; $^1H$ NMR ($CD_3OD$, 400 MHz) $\delta$: 7.57 (m, 1H), 5.60 (d, $J$ = 5.7, 1H), 3.95 (d, $J$ = 13.0 Hz, 1H), 3.91 (d, $J$ = 13.0 Hz, 1H), 3.86 (d, $J$ = 10.2 Hz, 1H), 3.26 (t, $J$ = 5.7 Hz, 1H), 3.12 (t, $J$ = 2.8 Hz, 1H), 2.62 (p, $J$ = 7.0 Hz, 1H), 2.52 (d, $J$ = 19.0 Hz, 1H), 2.44 (d, $J$ = 19.0 Hz, 1H), 2.02 (dq, $J$ = 10.2, 6.5 Hz, 1H), 1.74 (dd, $J$ = 2.8, 1.4 Hz, 3H), 1.23 (s, 3H), 1.22 (s, 3H), 1.18 (d, $J$ = 7.0 Hz, 3H), 1.06 (d, $J$ = 6.5 Hz, 3H), and 1.02 (d, $J$ = 5.7 Hz, 1H); $^{13}C$ NMR ($CD_3OD$, 100 MHz) $\delta$: 210.5, 181.6, 161.0, 142.5, 134.4, 129.9, 79.7, 77.6, 74.8, 69.0, 68.1, 57.7, 46.2, 40.1, 38.6, 36.8, 35.5, 27.2, 24.3, 19.2, 19.1, 17.5, 15.5, and 10.2. Purity HPLC: 96.2%. HRMS (ESI): $m/z$ calcd for $C_{24}H_{34}O_7Na$ $[M + Na]^+$, 457.2202; found, 457.2200.

*Phorbol 13-Phenylacetate (**6**) (86%).* White amorphous solid; $[\alpha]_D^{21}$ + 4.4 ($c$ 1.4, $CHCl_3$). IR (KBr) $\upsilon_{máx}$: 3417, 2921, 2848, 1710, 1461, 1125, 1078, 1022, and 792 $cm^{-1}$. $^1H$ NMR ($CD_3OD$, 500 MHz) $\delta$: 7.55 (m, 1H), 7.35−7.21 (m, 5H), 5.55 (d, $J$ = 5.6 Hz, 1H), 3.94−3.88 (m, 3H), 3.71 (s, 2H), 3.23 (t, $J$ = 5.6 Hz, 1H), 3.10 (t, $J$ = 2.4 Hz, 1H), 2.50 (d, $J$ = 19.0 Hz, 1H), 2.43 (d, $J$ = 19.0 Hz, 1H), 2.01 (dq, $J$ = 10.5, 6.3 Hz, 1H), 1.73 (dd, $J$ = 2.9, 1.4 Hz, 3H), 1.18 (s, 3H), 1.05 (s, 3H), 1.04 (d, $J$ = 6.5 Hz, 3H), and 0.95 (d, $J$ = 5.5 Hz, 1H). $^{13}C$ NMR ($CD_3OD$, 125 MHz) $\delta$: 210.5, 176.5, 161.0, 142.5, 135.0, 134.4, 130.5 (2C), 129.8, 129.6 (2C), 128.3, 79.7, 77.5, 74.7, 69.7, 68.1, 57.7, 46.2, 42.2, 40.0, 38.6, 36.7, 27.3, 24.0, 17.4, 15.4, and 10.2. Purity HPLC: 96.8%. HRMS (ESI): $m/z$ calcd for $C_{28}H_{34}O_7Na$ $[M + Na]^+$, 505.2202; found, 505.2209.

*Phorbol 12-Phenylacetate-13-isobutyrate (**7**) (75%).* White amorphous solid; $[\alpha]_D^{21}$ + 10.0 ($c$ 5.1, $CHCl_3$). IR (KBr) $\upsilon_{máx}$: 3402, 2980, 2926, 2880, 1713, 1497, 1391, 1251, 1161, 988, and 757 $cm^{-1}$. $^1H$ NMR ($CD_3OD$, 500 MHz) $\delta$: 7.52 (m, 1H), 7.35−7.23 (m, 5H), 5.58 (d, $J$ = 5.5 Hz, 1H), 5.39 (d, $J$ = 10.5 Hz, 1H), 3.94 (d, $J$ = 13.0 Hz, 1H), 3.89 (d, $J$ = 13.0 Hz, 1H), 3.66 (s, 2H), 3.24 (t, $J$ = 5.5 Hz, 1H), 3.14 (t, $J$ = 2.4 Hz, 1H), 2.53 (m, 1H), 2.50−2.47 (m, 2H), 2.17 (dq, $J$ = 10.5, 4.0 Hz, 1H), 1.73 (dd, $J$ = 2.3, 1.6 Hz, 3H), 1.13 (d, $J$ = 1.9 Hz, 3H), 1.12 (d, $J$ = 1.9 Hz, 3H), 1.08 (s, 3H), 1.04 (s, 3H), 1.03 (d, $J$ = 5.1 Hz, 1H), and 0.84 (d, $J$ = 6.6 Hz, 3H). $^{13}C$ NMR ($CD_3OD$, 125 MHz) $\delta$: 208.8, 179.3, 171.9, 159.1, 141.4, 134.4, 133.1, 128.8 (2C), 128.2 (2C), 127.8, 126.7, 78.4, 77.4, 73.3, 66.5, 65.3, 55.8, 42.7, 41.1, 38.6, 37.0, 35.8, 34.1, 25.9, 22.6, 17.6, 17.5, 15.7, 13.3, and 8.8. Purity HPLC: 99.0%. HRMS (ESI): $m/z$ calcd for $C_{32}H_{30}O_8Na$ $[M + Na]^+$, 575.2621; found, 575.2639.

*Phorbol 12-Tigliate-13-isobutyrate (**8**) (79%).* Spectroscopic data of compound **8** were identical to those described in the literature.[35,36] Purity HPLC: 99.5%.

*Phorbol 12-Isobutyrate-13-phenylacetate (**9**) (52%).* White amorphous solid; $[\alpha]_D^{21}$ + 12.8 ($c$ 0.4, $CHCl_3$). IR (KBr) $\upsilon_{máx}$: 3430, 2924, 2854, 1710, 1457, 1376, and 787 $cm^{-1}$. $^1H$ NMR ($CD_3OD$, 400 MHz) $\delta$: 7.53 (br s, 1H), 7.32−7.22 (m, 5H), 5.58 (d, $J$ = 5.7 Hz, 1H), 5.47 (d, $J$ = 10.4 Hz, 1H), 3.94 (d, $J$ = 13.2 Hz, 1H), 3.89 (d, $J$ = 13.2 Hz, 1H), 3.67 (s, 2H), 3.26 (t, $J$ = 5.7 Hz, 1H), 3.14 (d, $J$ = 3.0 Hz, 1H), 2.57 (hept, $J$ = 7.0 Hz, 1H), 2.50 (d, $J$ = 19.0 Hz, 1H), 2.46 (d, $J$ = 19.0 Hz, 1H), 2.21 (dq, $J$ = 10.4, 6.4 Hz, 1H), 1.73 (dd, $J$ = 3.0, 1.3 Hz, 3H), 1.23 (s, 3H), 1.15 (d, $J$ = 7.0 Hz, 3H), 1.05 (d, $J$ = 5.7 Hz, 1H), 1.03 (s, 3H), and 0.88 (d, $J$ = 6.4 Hz, 3H). $^{13}C$ NMR ($CD_3OD$, 100 MHz) $\delta$: 210.3, 178.7, 175.7, 160.5, 142.9, 134.9, 134.6, 130.7 (2C), 129.5 (2C), 129.2, 128.2, 79.8, 78.2, 74.7, 67.9, 67.4, 57.3, 44.3, 42.1, 40.0, 38.4, 37.1, 35.4, 27.5, 24.0, 19.4, 19.2, 17.4, 14.8, and 10.2. Purity HPLC: 99.4%. HRMS (ESI): $m/z$ calcd for $C_{32}H_{39}O_8$ $[M - H]^-$, 551.2645; found, 551.2631.

**Plant Material.** Latex from *E. resinifera* was collected in November 2016 in Demnate, Beni Mellal-Khenifera Province (Marruecos) and was obtained by making repeated cuts along the branches of plants and collecting the white milky exudates. A vouch specimen has been kept at the herbarium of the chemistry laboratory of Natural Substances, Mohamed V University, Rabat (Morocco).


https://doi.org/10.1021/acs.jmedchem.1c00156
J. Med. Chem. 2021, 64, 6070−6084

**Extraction and Isolation.** Air-dried sample of *E. resinifera* latex (200 g) was macerated in EtOAc (200 mL, 3 times). The resulting solution was filtered first by filter paper strips and then through a short bed of TLC-grade silica gel (30 g). The yellowish extract, obtained after solvent removal, was magnetically stirred with acetonitrile in order to remove triterpene compounds (white precipitate). Acetonitrile fraction (yellow organic extract) was concentrated and subjected to purification by vacuum liquid chromatography over silica gel column using hexane/EtOAc gradient and $CH_3OH$ to yield six fractions (Fr1: 10%, Fr2-Fr4: 20, 30, and 50%, respectively, Fr5: 100% EtOAc, and Fr6: $CH_3OH$). The phorbol-containing fraction (Fr4) was purified by open-column chromatography using hexane/EtOAc (30:70−0:100, v/v) to obtain four subfractions which were analyzed by UHPLC−HRMS, taking into account the results of mass spectroscopy of our synthetic phorbol 12,13-diesters. A compound isomeric to phorbol 12-phenylacetate-13-isobutyrate (**7**) was detected in subfraction FR4-4 (58.1 mg), which was further chromatographed through analytic HPLC using Si-60 column and EtOAc/hexane (40% of EtOAc) as the solvent system. Finally, two compounds not described previously, 12-deoxy-16-hydroxyphorbol 13-phenylacetate-16-isobutyrate (DPPI, **10**, 1.0 mg, 0.0005%, 46.18 min) and 12-deoxy-16-hydroxyphorbol 13-phenylacetate-16-tigliate (DPPT, **11**, 1.4 mg, 0.0007%, 51.1 min), were isolated.

*12-Deoxy-16-hydroxyphorbol 13-Phenylacetate-16-isobutyrate (**10**).* White amorphous powder; $[\alpha]_D^{24}$ + 9.61 (*c* 0.08, $CH_3OH$); IR (KBr) $\upsilon_{máx}$: 3416, 1712, 1633, and 1100 $cm^{-1}$; for $^1H$ and $^{13}C$ NMR ($CD_3OD$) data, see Table 1. Purity HPLC: 99.0%. HRESIMS *m*/*z*: 575.2621 $[M + Na]^+$, calcd for $C_{32}H_{40}O_8Na$, 575.2621.

*12-Deoxy-16-hydroxyphorbol 13-Phenylacetate-16-tigliate (**11**).* White amorphous powder; $[\alpha]_D^{24}$ + 18.52 (*c* 0.14, $CH_3OH$); IR (KBr) $\upsilon_{máx}$: 3416, 2923, 1705, and 1269 $cm^{-1}$; for $^1H$ and $^{13}C$ NMR ($CD_3OD$) data, see Table 1. Purity HPLC: 98.2%. HRESIMS *m*/*z*: 587.2662 $[M + Na]^+$, calcd for $C_{33}H_{40}O_8Na$, 587.2621.

**Animals.** SVZ-derived NPCs were isolated from 7-day postnatal CD1 mice and used for *in vitro* experiments. For *in vivo* experiments, 2-month-old male CD1 mice were used. The animals were housed under controlled conditions of temperature (21−23 °C) and light (LD 12:12) with free access to food (AO4 standard maintenance diet, SAFE, Épinay-sur-Orge, France) and water. Care and handling of the animals were performed according to the Guidelines of the European Union Council (2010/63/EU) and the Spanish regulations (65/2012 and RD53/2013) for the use of laboratory animals. All studies involving animals are reported in accordance with the ARRIVE guidelines for reporting experiments involving animals.[37,38] The protocols used have been authorized by the Ethics Committee of the "Consejería de Agricultura, Pesca y Desarrollo sostenible" of the Junta de Andalucía", Spain, with the approval numbers 30/03/2016/038 and 04/03/2020/033.

**HEK293T Culture, Cloning, and Transfection.** HEK293T cells were obtained from ATCC (Manassas, VA, USA), cultured, transfected, and left overnight.[30] Thereafter, the cells were left in serum-free FluoroBrite DMEM (Thermo Fisher Scientific) for 30 min and used in time-lapse experiments as previously described.[39]

**Cloning of Human TGFα cDNA Fused to GFP and m-Cherry.** Full-length cDNA encoding the mCherry-TGFα-GFP construct containing the human TGFα (NCBI reference sequence: NM_003236.4) containing mCherry cDNA between nucleotides 126 and 127 of TGFα, and the enhanced green fluorescent protein (EGFP) in frame was designed and synthesized by GeneCust (Boynes, France) as previously described.[10]

**Time-Lapse Experiments and Fluorescence Analysis of mCherry-Fused TGFα or Neuregulin in the Culture Medium of HEK293T.** HEK293T cells were plated in μ−dishes (35 mm high, Ibidi, Munich, Germany). The cells were treated with different compounds, and images were taken during 3 h as described in the figure legends.

**SVZ-Derived NPC Isolation and Culture.** SVZ-derived cells were isolated following the same procedure described in Rabaneda et al.[40] For *in vitro* experiments in proliferation conditions, growth factors EGF and bFGF were used as indicated in the figure legends (see Supporting Information, Methods).

**Neurosphere Assay.** The effects of compounds **1**, **2**, **3**, **5**, and **11** were tested using neurosphere assays in order to evaluate NPC proliferation. This assay analyzes the size of the neurospheres formed after a period of time in the presence of increasing concentrations of the compounds added at the time of seeding. All experiments were performed in triplicates and a minimum of five independent times ($n$ = 5). The numbers and sizes of the neurospheres were measured as previously described[30] using ImageJ[41] (see Supporting Information, Methods).

**Intranasal Administration of Compounds 2 and 3.** Compounds were delivered intranasally as previously described.[42−44] Treatments were administered manually while the animal was placed standing with an extended neck.[44] A total of 12 μL of each solution was administered. 3 μL was delivered each time alternating both nasal cavities using a micropipette. Thereafter, the mouse was kept in such a position for 10 additional seconds to ensure complete inhalation of the fluid. Based on the results obtained *in vitro*, compound **3** was used at a concentration of 10 and 100 nM in saline, whereas compound **2** was used at 5 mM; saline was used as the vehicle. In all experiments, the mice were coded, and treatment (vehicle or compound) was assigned randomly to the code numbers and applied. Blind quantifications were performed to avoid subjective biases.[10]

**Brain Processing and Immunohistochemistry.** At the end of the treatment, brains were perfused with paraformaldehyde (PFA) and sliced using a cryotome into 30 μm sections. Immunohistochemistry was performed as previously described.[30,41,45] Antibodies used were rat monoclonal anti-BrdU (1:500, Abcam, Cambridge, UK) and rabbit monoclonal anti-DCX (1:500, Abcam, Cambridge, UK). The secondary antibodies used were donkey anti-rat IgG labeled with AlexaFluor 488 (1:1000) and donkey anti-rabbit IgG labeled with Alexa-Fluor 594 (1:1000) from Invitrogen (Carlsbad, CA).

**Quantification of Neurogenesis in Brain Sections.** Cells positive for BrdU and DCX in the SVZ were estimated as described.[40,45] Positive cells were quantified throughout the lateral and laterodorsal walls of the lateral ventricles in every fifth section; 6−8 sections per brain were analyzed by fluorescence microscopy at 20× magnification. Mice were coded depending on the treatment, and quantification of cells in brain slices was done in blinded analysis. Cells in the SVZ of both brain hemispheres have been quantified unless otherwise indicated.

**Molecular Docking.** The crystal structure (PDB: 1PTR)[27] of PKC Delta C1 domain complexed with phorbol 13-acetate (P13-Ac) and the full-length proteins PKCβII (PDB ID: 3PFQ)[31] were used to perform *in silico* analysis. To generate three-dimensional (3D) ligands, two-dimensional structures drawn by ChemDraw Ultra were superimposed on the crystal structure of P13-Ac using Forge 10.5.0 (Cresset BioMolecular Discovery LTD). All 3D ligands were verified using NOESY NMR data. Molecular docking analysis was carried out using AutoDockTools-1.5.6 (The Scripps Research Institute, La Jolla, CA, USA). The target protein regions were limited with a grid box of 40 × 40 × 40 Å that was centered ($x$ = 10.879, $y$ = 25.984, and $z$ = 25.53) on the binding site where P 13Ac was removed from the crystallized enzyme. The binding pocket residues of PKC-β were identified by comparison with the activator-binding residues of PKCδ-C1B. The residues selected were limited with grid box of 40 × 40 × 40 Å centered at ($x$ = −59.148, $y$ = 16.647, and $z$ = −5.326). The Lamarckian genetic algorithm was used to perform the automated molecular dockings with the preset parameters. The total number of genetic algorithm runs and iterations was set to 100 and 1.0 × $10^7$, respectively. The lowest binding energy conformation was selected for UCSF Chimera analysis. 3D protein−ligand interactions were visualized in Discovery Studio Visualizer.

## ■ ASSOCIATED CONTENT

### Supporting Information

The Supporting Information is available free of charge at https://pubs.acs.org/doi/10.1021/acs.jmedchem.1c00156.



https://doi.org/10.1021/acs.jmedchem.1c00156
J. Med. Chem. 2021, 64, 6070−6084

mCherry/GFP ratio remains unaltered in the absence of the compound (AVI)
mCherry/GFP ratio remains unaltered in the presence of 0.5 $\mu$M phorbol (AVI)
mCherry/GFP ratio on the addition of compound **3** (AVI)
mCherry/GFP ratio on the addition of compound **2** (AVI)
mCherry/GFP ratio on the addition of compound **5** (AVI)
Effect of addition of compound **10** on TGF$\alpha$ release (AVI)
Docking of DPPI with PKC$\beta$ (PDB)
Docking of DPPT with PKC$\beta$ (PDB)
Docking of DPA with PKC$\beta$ (PDB)
Docking of **7** with PKC$\beta$ (PDB)
Docking of **3** with PKC$\beta$ (PDB)
Docking of Phorbol with PKC$\beta$ (PDB)
Docking of DPB with PKC$\beta$ (PDB)
Molecular formula strings of tested compounds (CSV)
Structure of active phorbol derivatives; isolation of phorbol 20-trityl ether; NMR spectra of compounds **3**−**11**; HPLC chromatograms for compounds **2**−**11**; UPLC-HRMS-assisted identification of 12-deoxyphorbol 13,16-diesters from *E. resinifera*; proposed fragmentation route for selected ion on $MS^E$ spectrum for compounds **9**−**11**; effect of intranasal administration of compound **3**; physicochemical properties; docking analysis of phorbol derivatives; molecular docking of DPPT (**11**), DPPI (**10**), **7** and **3** and Phorbol (**1**), DPA and DPB on PKC$\delta$C1B; and molecular docking of DPPI (**10**) and DPPT (**11**), **7** and **3** and Phorbol (**1**), DPBand DPA on PKC$\delta$C1B (PDF)

## AUTHOR INFORMATION


### Corresponding Author

**Rosario Hernández-Galán** − *Departamento de Química Orgánica, Facultad de Ciencias and Instituto de Investigación en Biomoléculas (INBIO), Universidad de Cádiz, Puerto Real 11510, Cádiz, Spain; Instituto de Investigación e Innovación Biomédica de Cádiz (INIBICA), 11009 Cádiz, Spain;* orcid.org/0000-0003-1887-4796;
Email: rosario.hernandez@uca.es

### Authors

**Abdellah Ezzanad** − *Departamento de Química Orgánica, Facultad de Ciencias, Universidad de Cádiz, Puerto Real 11510, Cádiz, Spain*

**Ricardo Gómez-Oliva** − *Área de Fisiología, Facultad de Medicina, Universidad de Cádiz, 11002 Cádiz, Spain; Instituto de Investigación e Innovación Biomédica de Cádiz (INIBICA), 11009 Cádiz, Spain*

**Felipe Escobar-Montaño** − *Departamento de Química Orgánica, Facultad de Ciencias, Universidad de Cádiz, Puerto Real 11510, Cádiz, Spain*

**Mónica Díez-Salguero** − *Área de Fisiología, Facultad de Medicina, Universidad de Cádiz, 11002 Cádiz, Spain*

**Noelia Geribaldi-Doldan** − *Departamento de Anatomía y Embriología Humanas, Universidad de Cádiz, 11002 Cádiz, Spain*

**Samuel Dominguez-Garcia** − *Área de Fisiología, Facultad de Medicina, Universidad de Cádiz, 11002 Cádiz, Spain; Instituto de Investigación e Innovación Biomédica de Cádiz (INIBICA), 11009 Cádiz, Spain*

**José Manuel Botubol-Ares** − *Departamento de Química Orgánica, Facultad de Ciencias, Universidad de Cádiz, Puerto Real 11510, Cádiz, Spain; Instituto de Investigación e Innovación Biomédica de Cádiz (INIBICA), 11009 Cádiz, Spain;* orcid.org/0000-0002-2312-612X

**Carolina de los Reyes** − *Departamento de Química Orgánica, Facultad de Ciencias, Universidad de Cádiz, Puerto Real 11510, Cádiz, Spain*

**Rosa Durán-Patrón** − *Departamento de Química Orgánica, Facultad de Ciencias, Universidad de Cádiz, Puerto Real 11510, Cádiz, Spain; Instituto de Investigación e Innovación Biomédica de Cádiz (INIBICA), 11009 Cádiz, Spain;* orcid.org/0000-0002-5307-4164

**Pedro Nunez-Abades** − *Departamento de Fisiología, Facultad de Farmacia, Universidad de Sevilla, 41012 Sevilla, Spain*

**Antonio J. Macías-Sánchez** − *Departamento de Química Orgánica, Facultad de Ciencias and Instituto de Investigación en Biomoléculas (INBIO), Universidad de Cádiz, Puerto Real 11510, Cádiz, Spain; Instituto de Investigación e Innovación Biomédica de Cádiz (INIBICA), 11009 Cádiz, Spain;* orcid.org/0000-0001-6002-4977

**Carmen Castro** − *Area de Fisiología, Facultad de Medicina, Universidad de Cádiz, 11002 Cádiz, Spain; Instituto de Investigación e Innovación Biomédica de Cádiz (INIBICA), 11009 Cádiz, Spain*

Complete contact information is available at: https://pubs.acs.org/10.1021/acs.jmedchem.1c00156


### Author Contributions

The manuscript was written through the contributions of all authors. All authors have given approval to the final version of the manuscript.


### Funding

Ministerio de Ciencia, Innovación y Universidades (grant nos RTI2018−099908-B-C21, and RTI2018−099908-B-C22 MICINN/FEDER) and Consejería de Economía, Conocimiento, Empresas y Universidades Junta de Andalucía (grant no FEDER-ANDALUCÍA 2018−00106647).


### Notes

The authors declare no competing financial interest.

## ACKNOWLEDGMENTS


This work was supported by the Spanish Ministerio de Ciencia, Innovación y Universidades (grant nos RTI2018−099908-B-C21 and RTI2018−099908-B-C22 MICINN/FEDER granted to CC and RHG, respectively) and Consejería de Economía, Conocimiento, Empresas y Universidades Junta de Andalucía (grant no FEDER-ANDALUCÍA sol2018−00106647-tra). We thank the "Servicio de experimentación y producción animal (SEPA) de la Universidad de Cádiz" as well as the "Servicios Centrales de apoyo a la investigación en Ciencias de la Salud (SCICS) de la Universidad de Cádiz" and "Servicios centrales de Ciencia y tecnología (SC-ICYT) de la Universidad de Cádiz".


## ABBREVIATIONS

COSY, correlation spectroscopy.; DMAP, dimethylamino pyridine.; DPA, 12-deoxyphorbol 13-angelate; DPB, 12-deoxyphorbol 13-isobutyrate; DPP, 12-deoxyphorbol 13-phenylacetate; DPPI, 12-deoxy-16-hydroxy-13-phenylacetyl

phorbol 16-isobutyrate; DPPT, 12-deoxy-16-hydroxy-13-phenylacetyl phorbol 16-tigliate; EDCI, 1-ethyl-3-(3-dimethylaminopropyl)carbodiimide; EtOAc, ethyl acetate; HBA, hydrogen bond acceptor; HBD, hydrogen bond donator; HMBC, heteronuclear multiple−bond correlation; HMQC, heteronuclear multiple−quantum correlation; NOESY, nuclear overhauser effect spectroscopy; NPC, neural progenitor cell; PKC, protein kinase C; PMA, phorbol 12-mystirate 13-acetate; RP-HPLC, reverse phase-high-performance liquid chromatography; SAR, structure−activity relationships; TLC, thin layer chromatography; UHPLC−HRMS, ultrahigh-performance liquid chromatography-high-resolution mass spectrometry

## REFERENCES


(1) Fleminger, S.; Ponsford, J. Long term outcome after traumatic brain injury. *Br. Med. J.* **2005**, *331*, 1419−1420.

(2) Ratcliff, G.; Colantonio, A.; Escobar, M.; Chase, S.; Vernich, L. Long-term survival following traumatic brain injury. *Disability and rehabilitation* **2005**, *27*, 305−314.

(3) Schachar, R. J.; Park, L. S.; Dennis, M. Mental Health Implications of Traumatic Brain Injury (TBI) in Children and Youth. *Can. Acad. Child Adolesc. Psychiatr.* **2015**, *24*, 100−108.

(4) Doetsch, F.; García-Verdugo, J. M.; Alvarez-Buylla, A. Cellular composition and three-dimensional organization of the subventricular germinal zone in the adult mammalian brain. *J. Neurosci.* **1997**, *17*, 5046−5061.

(5) Gage, F. H.; Coates, P. W.; Palmer, T. D.; Kuhn, H. G.; Fisher, L. J.; Suhonen, J. O.; Peterson, D. A.; Suhr, S. T.; Ray, J. Survival and differentiation of adult neuronal progenitor cells transplanted to the adult brain. *Proc. Natl. Acad. Sci. U.S.A.* **1995**, *92*, 11879−11883.

(6) Carrasco, M.; Rabaneda, L. G.; Murillo-Carretero, M.; Ortega-Martínez, S.; Martínez-Chantar, M. L.; Woodhoo, A.; Luka, Z.; Wagner, C.; Lu, S. C.; Mato, J. M.; Micó, J. A.; Castro, C. Glycine N-methyltransferase expression in the hippocampus and its role in neurogenesis and cognitive performance. *Hippocampus* **2014**, *24*, 840−852.

(7) Hierro-Bujalance, C.; Del Marco, A.; Ramos-Rodriguez, J.; Infante-Garcia, C.; Gomez-Santos, S. B.; Herrera, M.; Garcia-Alloza, M. Cell proliferation and neurogenesis alterations in Alzheimer's disease and diabetes mellitus mixed murine models. *J. Neurochem.* **2020**, *154*, 673−692.

(8) Berdugo-Vega, G.; Arias-Gil, G.; López-Fernández, A.; Artegiani, B.; Wasielewska, JM.; Lee, C.-C.; Lippert, MT.; Kempermann, G.; Takagaki, K.; Calegari, F. Increasing neurogenesis refines hippocampal activity rejuvenating navigational learning strategies and contextual memory throughout life. *Nat. Commun.* **2020**, *11*, 1138.

(9) Geribaldi-Doldán, N.; Flores-Giubi, E.; Murillo-Carretero, M.; García-Bernal, F.; Carrasco, M.; Macías-Sánchez, AJ.; Domínguez-Riscart, J.; Verástegui, C.; Hernández-Galán, R.; Castro, C. 12-Deoxyphorbols promote adult neurogenesis by inducing neural progenitor cell proliferation via PKC activation. *Int. J. Neuropsychopharmacol.* **2016**, *19*, pyv085.

(10) Domínguez-García, S.; Gómez-Oliva, R.; Geribaldi-Doldán, N.; Hierro-Bujalance, C.; Sendra, M.; Ruiz, F. A.; Carrascal, L.; Macías-Sánchez, A. J.; Verástegui, C.; Hernández-Galán, R.; García-Alloza, M.; Nunez-Abades, P.; Castro, C. Effects of classical PKC activation on hippocampal neurogenesis and cognitive performance: mechanism of action. *Neuropsychopharmacology* **2021**, *46*, 1207. Epub ahead of print. PMID: 33335309

(11) Dang, M.; Armbruster, N.; Miller, M. A.; Cermeno, E.; Hartmann, M.; Bell, G. W.; Root, D. E.; Lauffenburger, D. A.; Lodish, H. F.; Herrlich, A. Regulated ADAM17-dependent EGF family ligand release by substrate-selecting signaling pathways. *Proc. Natl. Acad. Sci. U.S.A.* **2013**, *110*, 9776−9781.

(12) Dang, M.; Dubbin, K.; D'Aiello, A.; Hartmann, M.; Lodish, H.; Herrlich, A. Epidermal growth factor (EGF) ligand release by substrate-specific a disintegrin and metalloproteases (ADAMs) involves different protein kinase C (PKC) isoenzymes depending on the stimulus. *J. Biol. Chem.* **2011**, *286*, 17704−17713.

(13) Geribaldi-Doldán, N.; Gómez-Oliva, R.; Dominguez-Garcia, S.; Nunez-Abades, P.; Castro, C. Protein kinase C: targets to regenerate brain injuries? *Front Cell Dev. Biol.* **2019**, *7*, 7−39.

(14) Shi, Q.-W.; Su, X.-H.; Kiyota, H. Chemical and pharmacological research of the plants in genus euphorbia. *Chem. Rev.* **2008**, *108*, 4295−4327.

(15) Vasas, A.; Hohmann, J. Euphorbia diterpenes: isolation, structure, biological activity, and synthesis (2008−2012). *J. Chem. Rev.* **2014**, *114*, 8579−8612.

(16) Hecker, E.; Schmidt, R. Phorbolesters—the Irritants and Cocarcinogens of Croton Tiglium L. *Fortschr. Chem. Org. Naturst.* **1974**, *31*, 377−467.

(17) Gschwendi, M.; Hecker, E. Biologically active compounds of Euphorbiaceae. I. Skin irritant and cocarcinogenic factors from Euphorbia cooperi. *Z. Krebsforsch. Klin. Onkol.* **1973**, *80*, 335−350.

(18) Hergenhahn, M.; Kusumoto, S.; Hecker, E. On the active principles of the spurge family (Euphorbiaceae). *J. Canc. Res. Clin. Oncol.* **1984**, *108*, 98−109.

(19) Hergenhahn, M.; Fuerstenberger, G.; Opferkuch, H. J.; Adolf, W.; Mack, H.; Hecker, E. Biological assays for irritant tumor-initiating and -promoting activities. I. Kinetics of the irritant response in relation to the initiation-promoting activity of polyfunctional diterpenes representing tigliane and some daphnane types. *J. Canc. Res. Clin. Oncol.* **1982**, *104*, 31−39.

(20) Bertolini, T. M.; Giorgione, J.; Harvey, D. F.; Newton, A. C. Protein kinase C translocation by modified phorbol esters with functionalized lipophilic regions. *J. Org. Chem.* **2003**, *68*, 5028−5036.

(21) Jacobi, P.; Härle, E.; Schairer, H. U.; Hecker, E. Zur Chemie des Phorbols, XVI. 4α-Phorbol. *Liebigs Ann. Chem.* **1970**, *741*, 13−32.

(22) Tseng, S.-S.; Van Duuren, B. L.; Solomon, J. J. Synthesis of 4α-phorbol 9-myristate 9a-acetate and related esters. *J. Org. Chem.* **1977**, *42*, 3645.

(23) Plumb, R. S.; Johnson, K. A.; Rainville, P.; Smith, B. W.; Wilson, I. D.; Castro-Perez, J. M.; Nicholson, J. K. UPLC/MS$^{E}$; a new approach for generating molecular fragment information for biomarker structure elucidation. *Rapid Commun. Mass Spectrom.* **2006**, *20*, 1989−1994.

(24) Nothias-Scaglia, L. F.; Schmitz-Afonso, I.; Renucci, F.; Roussi, F.; Touboul, D.; Costa, J.; Litaudon, M.; Paolini, J. Insights on profiling of phorbol, deoxyphorbol, ingenol and jatrophane diterpene esters by high performance liquid chromatography coupled to multiple stage mass spectrometry. *J. Chromatogr. A* **2015**, *1422*, 128−139.

(25) Vogg, G.; Achatz, S.; Kettrup, A.; Sandermann, H. Fast, sensitive and selective liquid chromatographic−tandem mass spectrometric determination of tumor-promoting diterpene esters. *J. Chromatogr. A* **1999**, *855*, 563−573.

(26) Santiskulvong, C.; Rozengurt, E. Protein kinase C alpha mediates feedback inhibition of EGF receptor transactivation induced by Gq-coupled receptor agonists. *Cell Signal.* **2007**, *19*, 1348−1357.

(27) Zhang, G.; Kazanietz, M. G.; Blumberg, P. M.; Hurley, J. H. Crystal structure of the Cys2 activator-binding domain of protein kinase Cδ in complex with phorbol ester. *Cell* **1995**, *81*, 917−924.

(28) Newton, A. C. Protein kinase C: perfectly balanced. *Crit. Rev. Biochem. Mol. Biol.* **2018**, *53*, 208−230.

(29) Das, J.; Rahman, G. M. C1 Domains: Structure and Ligand-Binding Properties. *Chem. Rev.* **2014**, *114*, 12108−12131.

(30) Murillo-Carretero, M.; Geribaldi-Doldan, N.; Flores-Giubi, E.; Garcia-Bernal, F.; Navarro-Quiroz, E. A.; Carrasco, M.; Macías-Sánchez, A. J.; Herrero-Foncubierta, P.; Delgado-Ariza, A.; Verástegui, C.; Domínguez-Riscart, J.; Daoubi, M.; Hernández Galán, R.; Castro, C. ELAC (3,12-di-O-acetyl-8-O-tigloilingol), a plant-derived lathyrane diterpene, induces subventricular zone neural progenitor cell proliferation through PKCbeta activation. *Br. J. Pharmacol.* **2017**, *174*, 2373−2392. Erratum in: *Br J. Pharmacol.* **2020**, *177*, 235.




https://doi.org/10.1021/acs.jmedchem.1c00156
J. Med. Chem. 2021, 64, 6070−6084

(31) Leonard, T. A.; Różycki, B.; Saidi, L. F.; Hummer, G.; Hurley, J. H. Crystal structure and allosteric activation of protein kinase C βII. *Cell* **2011**, *144*, 55−66.
(32) Appendino, G.; Cravotto, G.; Palmisano, G.; Annunziata, R.; Szallasi, A. Synthesis and evaluation of phorboid 20-homovanillates: discovery of a class of ligands binding to the vanilloid (capsaicin) receptor with different degrees of cooperativity. *J. Med. Chem.* **1996**, *39*, 3123−3131.
(33) Appendino, G.; Bertolino, A.; Minassi, A.; Annunziata, R.; Szallasi, A.; de Petrocellis, L.; Di Marzo, V. Synthesis and biological evaluation of phorbol-resiniferatoxin (RTX) hybrids. *Eur. J. Org Chem.* **2004**, *2004*, 3413−3421.
(34) Szczepanski, C. V.; Schairer, H.-U.; Gschwendt, M.; Hecker, E. Zur chemie des phorbols, III. Mono- und diacetate des phorbols. *Justus Liebigs Ann. Chem.* **1967**, *705*, 199−210.
(35) Marshall, G. T.; Kinghorn, A. D. Short-chain phorbol ester constituents of croton oil. *J. Am. Oil Chem. Soc.* **1984**, *61*, 1220−1225.
(36) Zhang, X. L.; Wang, L.; Li, F.; Yu, K.; Wang, M. K. Cytotoxic Phorbol esters of croton tiglium. *J. Nat. Prod.* **2013**, *76*, 858−864.
(37) Kilkenny, C.; Browne, W.; Cuthill, I. C.; Emerson, M.; Altman, D. G. Animal research: reporting *in vivo* experiments: the ARRIVE guidelines. *Br. J. Pharmacol.* **2010**, *160*, 1577−1579.
(38) McGrath, J.; Drummond, G.; McLachlan, E.; Kilkenny, C.; Wainwright, C. Guidelines for reporting experiments involving animals: the ARRIVE guidelines. *Br. J. Pharmacol.* **2010**, *160*, 1573−1576.
(39) Gómez-Oliva, R.; Geribaldi-Doldán, N.; Domínguez-García, S.; Carrascal, L.; Verástegui, C.; Nunez-Abades, P.; Castro, C. Vitamin D deficiency as a potential risk factor for accelerated aging, impaired hippocampal neurogenesis and cognitive decline: a role for Wnt/β-catenin signaling. *Aging* **2020**, *12*, 13824−13844.
(40) Rabaneda, L. G.; Geribaldi-Doldán, N.; Murillo-Carretero, M.; Carrasco, M.; Martínez-Salas, J. M.; Verástegui, C.; Castro, C. Altered regulation of the Spry2/Dyrk1A/PP2A triad by homocysteine impairs neural progenitor cell proliferation. *Biochim. Biophys. Acta* **2016**, *1863*, 3015−3026.
(41) García-Bernal, F.; Geribaldi-Doldan, N.; Domínguez-García, S.; Carrasco, M.; Murillo-Carretero, M.; Delgado-Ariza, A.; Díez-Salguero, M.; Verástegui, C.; Castro, C. Protein kinase C inhibition mediates neuroblast enrichment in mechanical brain injuries. *Front. Cell. Neurosci.* **2018**, *12*, 462.
(42) Thorne, R. G.; Pronk, G. J.; Padmanabhan, V.; Frey, W. H. Delivery of insulin-like growth factor-I to the rat brain and spinal cord along olfactory and trigeminal pathways following intranasal administration. *Neuroscience* **2004**, *127*, 481−496.
(43) Francis, G. J.; Martinez, J. A.; Liu, W. Q.; Xu, K.; Ayer, A.; Fine, J.; Tuor, U. I.; Glazner, G.; Hanson, L. R.; Frey, W. H., 2nd; Toth, C. Intranasal insulin prevents cognitive decline, cerebral atrophy and white matter changes in murine type I diabetic encephalopathy. *Brain* **2008**, *131*, 3311−3334.
(44) Marks, D. R.; Tucker, K.; Cavallin, M. A.; Mast, T. G.; Fadool, D. A. Awake intranasal insulin delivery modifies protein complexes and alters memory, anxiety, and olfactory behaviors. *J. Neurosci.* **2009**, *29*, 6734−6751.
(45) Rabaneda, L. G.; Carrasco, M.; López-Toledano, M. A.; Murillo-Carretero, M.; Ruiz, F. A.; Estrada, C.; Castro, C. Homocysteine inhibits proliferation of neuronal precursors in the mouse adult brain by impairing the basic fibroblast growth factor signaling cascade and reducing extracellular regulated kinase 1/2-dependent cyclin E expression. *FASEB J.* **2008**, *22*, 3823−3835.


https://doi.org/10.1021/acs.jmedchem.1c00156
*J. Med. Chem.* 2021, 64, 6070−6084